

Polyelectrolyte-Based Capacitors and Transistors

Oscar Larsson

Norrköping 2011

Polyelectrolyte-Based Capacitors and Transistors

Oscar Larsson

Linköping Studies in Science and Technology. Dissertations, No. 1370

Copyright ©, 2011, Oscar Larsson, unless otherwise noted

ISBN: 978-91-7393-160-1

ISSN: 0345-7524

Printed by LiU-Tryck, Linköping, Sweden 2011

Cover: The capacitance and the phase angle versus frequency for a polyelectrolyte capacitor.

Abstract

Polymers are very attractive materials that can be tailored for specific needs and functionalities. Based on their chemical structure, they can for instance be made electrically insulating, semiconducting or conducting with specific mechanical properties. Polymers are often processable from a solution, which enables the use of conventional low-cost and high-volume manufacturing techniques to print electronic devices onto flexible substrates. A multitude of polymer-based electronic and electrochemical devices and sensors have been developed, of which some already has reached the consumer market.

This thesis focuses on polarization characteristics in polyelectrolyte-based capacitor structures and their role in sensors, transistors and supercapacitors. The fate of the ions in these capacitor structures, within the polyelectrolyte and at the interfaces between the polyelectrolyte and various electronic conductors (a metal, a semiconducting polymer or a network of carbon nanotubes), is of outermost importance for the device function. The humidity-dependent polarization characteristics in a polyelectrolyte capacitor are used as the sensing probe for wireless readout of a passively operated humidity sensor circuit. This sensor circuit can be integrated into a printable low-cost passive sensor label. By varying the humidity level, limitations and possibilities are identified for polyelectrolyte-gated organic field-effect transistors. Further, the effect of the ionic conductivity is investigated for polyelectrolyte-based supercapacitors. Finally, by using an ordinary electrolyte instead of a polyelectrolyte and a high-surface area (supercapacitor) gate electrode, the device mechanisms proposed for electrolyte-gated organic transistors are unified.

Populärvetenskaplig sammanfattning

Polymerer, eller plaster, är tilltalande material tack vare att dess egenskaper lätt kan skräddarsys för önskad funktion och behov redan under framställningen. Beroende på dess kemiska struktur kan polymererna besitta specifika mekaniska egenskaper och kan antingen göras elektriskt isolerande, halvledande eller ledande. Mängder av polymerbaserade elektroniska och elektrokemiska komponenter och sensorer har utvecklats. En del av dessa komponenter och tillhörande applikationer har redan nått marknaden och används flitigt i mobila kommunikationsprodukter. Polymerer kan även tillverkas från en lösning vilket gör det möjligt att använda traditionell tryckteknologi för att, i stora volymer och till ett lågt pris, trycka elektronik på flexibla substrat. Sådana tryckta elektronikkomponenter och kretsar bör drivas med låga spänningar för att vara kompatibla med t.ex. enkla tryckbara batterier. En framgångsrik väg mot komponenter som drivs med låga spänningar involverar elektrolyter.

Den här avhandlingen är inriktad mot polarisationskaraktäristiken i polyelektrolytbaserade kapacitansstrukturer, med fokus på dess roll i sensorer, transistorer och superkondensatorer. Jonernas beteende i dessa strukturer är av stor vikt för komponentfunktionen; dels hur de uppträder i elektrolyten men även deras karaktäristik vid gränssnittet mellan elektrolyten och olika elektroniska ledare (en metall, en halvledande polymer eller ett nätverk av kolnanorör). Polarisationskaraktäristiken i en polyelektrolytbaserad kondensator beror av fukt vilket kan användas för att detektera luftfuktighet i en sensorkrets, vilken i sin tur kan avläsas med trådlös överföring. Denna sensorkrets har fördelen att den inte behöver något eget batteri och har dessutom möjlighet att kunna integreras till en tryckbar sensoretikett vilken kan tillverkas till en låg kostnad. Vidare, grundläggande komponentegenskaper har studerats och etablerats i organiska transistorer, vilka styrs via polyelektrolyter, genom att variera fukthalten i dessa. Dessutom har jonledningsförmågens betydelse för polyelektrolytbaserade superkondensatorer undersökts. I slutet av avhandlingen sammanförs komponentmekanismer för att förklara funktionen i elektrolytbaserade organiska transistorer.

Acknowledgements

Without the help and support from many people in my surrounding, both at work and in private, this thesis would not have been a reality. Specifically, I would like to express my sincere gratitude to:

Xavier Crispin, my supervisor. Thank you for all your help, encouragement and support and for believing in me all these years. Also, I am grateful that you convinced me to do the “extra experiments”. I was not always positive to these experiments, but I have to admit that they for sure have improved the quality of my research.

Magnus Berggren, my co-supervisor, for opening up my eyes for organic electronics during my undergraduate studies and for later giving me the opportunity to work and study in the Organic Electronics group. Thank you for your support and encouragement since then.

Sophie, for making everything related to administration so easy for me.

Brains & Bricks, which is a research center within Linköping University for high-technology constructions, for financing part of my research. This center was initiated by Peab, Linköping University and Katrineholms kommun; special thanks to **Lars, Hans, Roger, Jan, Peter, Erik, Conny** and **Stefan**.

Ari, for all help and your contribution to my last project, and for valuable discussions.

Grace Wee, for introducing me into the world of supercapacitors and for our fruitful supercapacitor collaboration.

The entire **Organic Electronics** group, both past and present group members, for your friendship and help, and for creating such a nice working environment. Especially, I would like to thank: **Nate**, my previous co-supervisor, for your support at that time, **David** and **PeO** for introducing me into the field of organic electronics, **Lars** for the many discussions related to details and for giving me valuable comments on various subjects, **Klas** for all fun discussions and the help related to mathematical modeling, **Daniel** for the help with various language-related issues, and, **Kristin** and **Maria** for the support and all fun conversations.

Joakim, I am very thankful for the support and advices you still are giving me even if you now live “far away”. Thanks for being such a great friend.

My mother and father, **Ewa** and **Göran**, and my brother, **Victor**, for your support and for always being there. Thank you for ALL your help!

Finally, I would like to thank the most important persons in my life – my family: **Anna**, the love of my life, who has supported me more than I can describe. Thank you for your never-ending support, for always believing in me and for taking care of everything. **Oliver** and **Alva**, all your love, energy and happiness help me realize what really is important.

List of included papers

Paper 1:

Proton motion in a polyelectrolyte: A probe for wireless humidity sensors

Oscar Larsson, Xiaodong Wang, Magnus Berggren and Xavier Crispin

Sensors and Actuators, B: Chemical **2010**, *143*, 482-486

Contribution: All experimental work and circuit design. Wrote the first draft of the manuscript and was involved in the final editing and submission of the manuscript.

Paper 2:

Effects of the ionic currents in electrolyte-gated organic field-effect transistors

Elias Said, Oscar Larsson, Magnus Berggren and Xavier Crispin

Advanced Functional Materials **2008**, *18*, 3529-3536

Contribution: Part of experimental work. Wrote part of the first draft of the manuscript.

Paper 3:

Insulator polarization mechanisms in polyelectrolyte-gated organic field-effect transistors

Oscar Larsson, Elias Said, Magnus Berggren and Xavier Crispin

Advanced Functional Materials **2009**, *19*, 3334-3341

Contribution: All experimental and model-related work. Wrote the first draft of the manuscript and was involved in the final editing and submission of the manuscript.

Paper 4:

Effect of the ionic conductivity on the performance of polyelectrolyte-based supercapacitors

Grace Wee*, Oscar Larsson*, Madhavi Srinivasan, Magnus Berggren, Xavier Crispin and Subodh Mhaisalkar

Advanced Functional Materials **2010**, *20*, 4344-4350

* Equal contribution

Contribution: All experimental work together with G. Wee. Wrote the first draft of the manuscript together with G. Wee and was involved in the final editing of the manuscript.

Paper 5:

Unifying electrochemical and field-effect mechanisms in electrolyte-gated organic field-effect transistors

Oscar Larsson, Ari Laiho, Magnus Berggren and Xavier Crispin

Submitted

Contribution: All experimental work. Wrote the first draft of the manuscript and was involved in the final editing and submission of the manuscript.

Related work not included in this thesis

PEDOT:PSS-based electrochemical transistors for ion-to-electron transduction and sensor signal amplification

M. Berggren, R. Forchheimer, J. Bobacka, P.-O. Svensson, D. Nilsson, O. Larsson and A. Ivaska

Book chapter in *Organic Semiconductors in Sensor Applications*, edited by D. A. Bernards, R. M. Owens and G. G. Malliaras, Springer, 2008.

Polyelectrolyte-gated organic field-effect transistors

X. Crispin, L. Herlogsson, O. Larsson, E. Said and M. Berggren

Book chapter in *Iontronics – Ionic Carriers in Organic Electronic Materials and Devices*, edited by J. Leger, M. Berggren and S. Carter, Taylor & Francis Group, 2011.

Moister sensor

EP2275806, US20110011179

Device for integrating and indicating a parameter over time

EP2120107, US20090303041

Table of contents

1. INTRODUCTION	1
1.1. POLYMER ELECTRONICS	1
1.2. AIM AND OUTLINE OF THE THESIS.....	2
2. MATERIALS	5
2.1. SEMICONDUCTING POLYMERS	5
2.1.1. <i>Molecular structure</i>	5
2.1.2. <i>Electronic charge carriers and charge transport</i>	8
2.2. CARBON NANOTUBES	10
2.2.1. <i>Molecular structure</i>	10
2.2.2. <i>Carbon nanotube networks</i>	11
2.3. POLYMER-BASED ELECTROLYTES.....	12
2.3.1. <i>Polymer electrolytes</i>	12
2.3.2. <i>Polyelectrolytes</i>	12
2.3.3. <i>Ionic charge transport</i>	13
3. IMPEDANCE SPECTROSCOPY	15
3.1. BASIC PRINCIPLES	15
3.2. COMMON EQUIVALENT CIRCUITS	19
3.2.1. <i>The Debye equivalent circuit</i>	19
3.2.2. <i>The Cole-Cole equivalent circuit</i>	20
3.2.3. <i>The Randles equivalent circuit</i>	20
4. POLARIZATION IN CAPACITOR STRUCTURES	23
4.1. POLARIZATION IN CAPACITORS BASED ON DIELECTRIC MATERIALS.....	23
4.2. POLARIZATION IN CAPACITORS BASED ON ELECTROLYTES	25
5. DEVICES	29
5.1. POLYMER-BASED HUMIDITY SENSORS	29
5.1.1. <i>Resistive- and capacitive-type sensors</i>	29
5.1.2. <i>Wireless readout and sensing of passive resonance sensor circuits</i>	30
5.2. ORGANIC FIELD-EFFECT TRANSISTORS	33
5.2.1. <i>Device operation</i>	33
5.2.2. <i>Organic field-effect transistors operated at low voltages</i>	36
5.3. SUPERCAPACITORS.....	37
5.3.1. <i>Electric double layer capacitors</i>	39
5.3.2. <i>Pseudo-capacitors</i>	40
5.3.3. <i>Hybrid capacitors</i>	42
6. CONCLUSIONS AND FUTURE OUTLOOK	45
REFERENCES	49

Background

1. Introduction

1.1. Polymer electronics

Polymers are found in almost every product today. That is due to the wide variety of properties of different polymers. Their mechanical and thermal properties can be tailored by modifying the building blocks (the monomers) and the bonding scheme of the polymers. Polymers can, for instance, be made soft and flexible or hard and brittle. They can also be processed from a solution. Traditionally, polymers have been considered as electrically insulating materials and are for instance used as the insulating material around electrical conductors. This view of polymers, as electrically insulating, was changed with the discovery of conducting polymers in the late 1970s by Alan J. Heeger, Alan G. MacDiarmid and Hideki Shirakawa for which they were awarded the Nobel Prize in Chemistry “*for the discovery and development of electrically conductive polymers*” the year 2000 [1].

This discovery allows for new materials that combine the mechanical properties and the processing advantages of polymers with the electrical and optical properties of metals or semiconductors [2]. As an example; semiconducting polymers can be processed from a solution, which enables the use of low-cost and high-volume manufacturing techniques, such as roll-to-roll printing, to produce electronic devices onto flexible substrates. This is in strong contrast to the expensive and complex manufacturing techniques that are used in the traditional semiconductor industry today. Examples of polymer-based electronic devices that have been developed are light-emitting diodes [3, 4], field-effect transistors [5-7] and solar cells [8]. Polymer-based electrochemical devices include transistors [9] and logics [10], light-emitting electrochemical cells [11, 12], display cells [13, 14] and supercapacitors [15, 16]. Further, since the chemical and physical properties of polymers can be tailored for specific requirements, both conducting and non-conducting polymers have gained importance in the field of sensors [17]. Examples of polymer-based sensors that have been reported include humidity sensors [18, 19], biosensors [20] and ion-selective sensors [21, 22].

1.2. Aim and outline of the thesis

The possibility to manufacture electronics from a solution onto flexible substrates, such as paper or (insulating) plastics, opens up new opportunities for electronics. It enables low-cost electronic applications, components that so far have been too expensive to realize with traditional inorganic electronics, to now be manufactured with conventional high-volume printing techniques. The driving voltage to power such printed electronic devices and circuitry should typically be very low, ideally around 1 V or so to enable powering from, for instance, simple batteries, supercapacitors or solar cells. One successful route towards low-voltage operated electronic devices involves the usage of electrolytes. The scientific aim of my research has been to understand the polarization characteristics in polyelectrolyte-based capacitor structures, formed with a combination of metal, semiconducting polymer and network of carbon nanotubes electrodes; and their role in electronic devices envisioned for printed electronics. The results of my research are summarized in five papers (Paper 1-5).

Paper 1 is a first result of a product-related research project initiated by *Brains & Bricks*, a research center for high-technology constructions. Since humidity has been identified as a major problem in the construction industry, the long-term goal within the project is to develop a low-cost sensor concept for wireless readout of the humidity level inside constructed systems. Each sensor should be so inexpensive to produce that it becomes affordable to permanently mount several such sensors, as humidity sensor labels, inside a wall or beneath a floor, for instance. This would enable wireless monitoring of eventual moisture or leakage problems during and after the construction process. Paper 1 introduces a sensor concept for wireless readout in which the humidity-dependent ionic motion in a polyelectrolyte capacitor is used as the sensing probe.

Very high electric fields can be established at semiconducting polymer-electrolyte interfaces as such material systems are exposed to an electric addressing signal. This enables electrolyte-gated organic transistors to be operated at low voltages (< 2 V) even though the gate-insulating electrolyte layer is rather thick [23, 24]. This makes this class of transistors attractive for printed electronics applications. While the usage of some electrolytes clearly results in an electrochemical reaction in the bulk of the semiconducting polymer transistor channel [25], thus classifying such transistors as organic electrochemical transistors, the usage of a polyelectrolyte as gate insulator has been claimed to result in an organic field-effect transistor [24, 26]. Paper 2 focuses on the ionic current paths between the three terminals in

such transistors, while the polarization mechanisms of the polyelectrolyte gate insulator are investigated in Paper 3. Paper 5 unifies the mechanisms proposed for electrolyte-gated organic transistors, operating either as field-effect or electrochemical transistors. To be able to do that, an ordinary electrolyte is used instead of a polyelectrolyte and the gate electrode is a supercapacitor electrode.

Printed electronics applications are envisaged to be powered with printed energy storage devices, such as printed batteries or supercapacitors [27]. The electrolytes used in these printed energy sources should preferably be solid electrolytes in order to be compatible with common manufacturing processes. In Paper 4, a supercapacitor that is based on a solid polyelectrolyte is reported. This paper focuses on the effect of the ionic conductivity and its effect on the supercapacitor device performance.

The first part of the thesis provides the background information that is necessary to understand the scientific results included in the second part. The *Background* part, which is an extension and development of my licentiate thesis [28], starts with an introduction to semiconducting polymers, carbon nanotubes and polymer-based electrolytes, material characterization with impedance spectroscopy and polarization characteristics in polymer-based materials. That is followed by device principles related to the included papers. Finally, conclusions are outlined together with a future outlook.

2. Materials

2.1. Semiconducting polymers

2.1.1. Molecular structure

Polymers are macromolecules that are built up from a large number of repeated units, monomers, connected through covalent bonds. In organic polymers the repeating unit(s) includes carbon atoms, which have the ability to bond with other carbon atoms to form chains. The electronic ground state configuration of an isolated carbon atom is $1s^2 2s^2 2p^2$. In the presence of atoms surrounding the carbon atom, the atomic orbitals of the valence electrons will be distorted and can instead be described with a set of hybrid orbitals. In a set of hybrid orbitals, each hybrid orbital has identical shape and energy but they are oriented in different directions.

The carbon atoms forming the skeleton of conventional polymers are sp^3 hybridized. The valence electrons of such a carbon atom are described with four hybrid orbitals, which can be found as linear combinations of the 2s and the three 2p atomic orbitals, forming a tetrahedral-shaped structure with an angle of about 109° between the hybrid orbitals. Each of the hybrid orbitals forms a single bond to a neighboring atom through σ -bonding. For a carbon atom in polyethylene, two of these four σ bonds are formed with adjacent carbon atoms while the remaining two σ bonds are formed with hydrogen atoms, see Figure 2.1a. The electrons involved in the σ bonds along the carbon backbone are strongly localized between the atoms that they hold together. This results in a large energy difference between the highest occupied molecular orbital (HOMO) and the lowest unoccupied molecular orbital (LUMO), in other words a large energy gap $E_g(\sigma)$, rendering these materials electrically insulating and transparent (Fig. 2.1b).

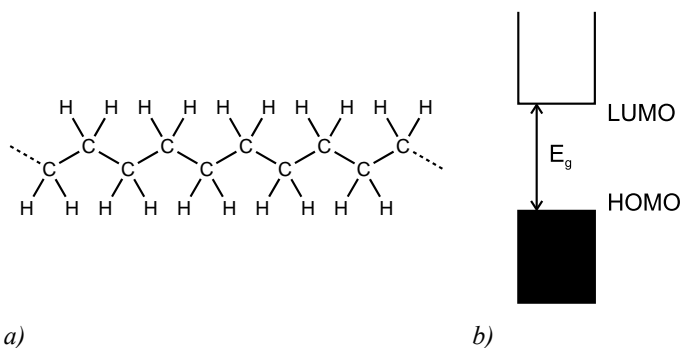


Figure 2.1. a) The molecular structure of polyethylene, and b) the large energy gap (E_g) between the HOMO and the LUMO.

In contrast to conventional insulating polymers each backbone carbon atom in a semiconducting polymer is sp^2 hybridized. For such a carbon atom, three of the four valence electrons are described with hybrid orbitals. These three hybrid orbitals, which can be found as linear combinations of the 2s and two of the three 2p atomic orbitals, form a planar structure with an angle of 120° between the hybrid orbitals. The hybrid orbitals form σ bonds to neighboring atoms and create the backbone of the polymer. Like the electrons involved in the σ bonds along the carbon backbone of conventional polymers, the electrons involved in these σ bonds are strongly localized between the atoms that they hold together, leading to a large energy gap between the filled σ band and the empty σ^* band. The remaining valence electron, not participating in the sp^2 hybridization, is described with a 2p atomic orbital oriented perpendicular to the planar structure defined by the hybrid orbitals. When the 2p atomic orbitals of two adjacent carbon atoms overlap sideways they combine into two molecular orbitals, one π bonding molecular orbital and one π^* anti-bonding molecular orbital. Along the backbone of a semiconducting polymer chain that consists of N sp^2 hybridized carbon atoms (each contributes to a singly occupied 2p atomic orbital) there are a total of N 2p atomic orbitals that combine into N molecular orbitals with different discrete energy levels. In the electronic ground state, because each molecular orbital is capable of containing two spin-paired electrons, the $N/2$ lowest energy states, corresponding to the π bonding molecular orbitals, will be occupied leaving the higher-energy π^* anti-bonding molecular orbitals empty.

For large values of N , as for polymers, the discrete energy levels become so closely spaced that they can be considered as a continuous energy band. If the π overlap of all adjacent 2p

atomic orbitals would be equal, meaning that the bonds between every carbon atom would have equal length, the π electrons would be completely delocalized along the backbone. The resulting energy band would then be half-filled and the polymer should behave as a one-dimensional metal. However, the energy of the system can be lowered by increasing the density of π electrons between every other carbon atom to create a π bond in addition to a σ bond, that is a double bond. By this introduction of alternating single and double bonds, or alternating long and short bonds, an energy gap is created, see Figure 2.2. This situation is described more generally by Peierls' theorem, which claims that a one-dimensional metal is always unstable with respect to a geometry modification that lowers the symmetry. The one-dimensional metallic structure of semiconducting polymers is thus not stable and undergoes a distortion, such as a bond alternation. As a result, a band gap $E_g(\pi)$ is opened up between the filled π band and the empty π^* band. The band gap of semiconducting polymers tends to be in the range 1.5-3 eV [29], which corresponds to the same range as inorganic semiconductors. With inorganic semiconductor terminology the completely filled π band is referred to as the valence band while the completely empty π^* band is referred to as the conduction band. In Figure 2.3 the molecular structures of different semiconducting polymers are displayed, note the pattern of alternating single and double bonds.

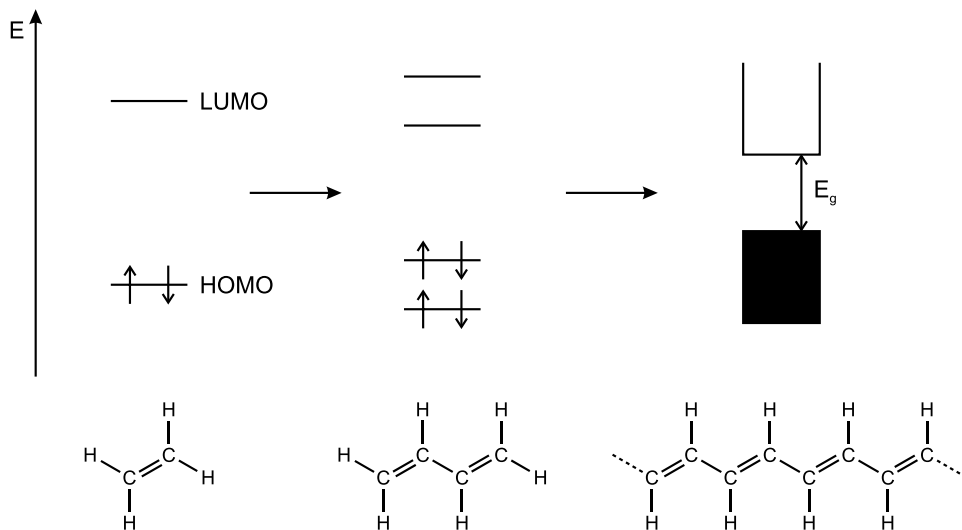


Figure 2.2. Electronic structures of molecules with sp^2 hybridized carbon atoms. The $2p$ atomic orbital of each carbon atom combines into molecular orbitals. For polymers (right), the discrete energy levels become so closely spaced that they can be considered as continuous energy bands.

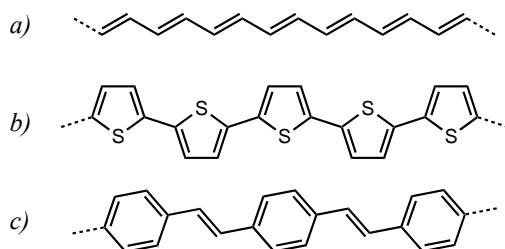


Figure 2.3. Molecular structures (short-hand notation) of three different semiconducting polymers. In a) polyacetylene, b) polythiophene, and c) polyphenylenevinylene.

2.1.2. Electronic charge carriers and charge transport

For a semiconducting polymer to be able to conduct electronic current, charge carriers must be introduced into the polymer. These charge carriers can be introduced via chemical or electrochemical doping, or via charge-injection. Most semiconducting polymers have a non-degenerate ground state with a preferred single and double bond alternation. The overall energy of non-degenerate ground state polymers depend on the bond alternation where the quinoid bonding configuration corresponds to a higher energy state compared to the aromatic bonding configuration. Charges (holes or electrons) introduced into such semiconducting polymers are stabilized by a local rearrangement of the bonding alternation in the vicinity of the charge. The charge together with the distortion of the bonding configuration is called a polaron and is delocalized over a small segment of the chain, see Figure 2.4. The formation of a polaron results in new localized states in the band gap. Polarons are singly charged, carry half-integral spin and can be either positive or negative.

Upon further addition of charges, polarons might combine. This result in two charges coupled to each other via a local rearrangement of the bonding alternation, this combination of charges coupled with the distortion of the bonding configuration is called a bipolaron. A bipolaron is doubly charged, carries no spin and can be either positive or negative. The formation of a bipolaron can be more favorable compared to the formation of two separate polarons; this is often the case in the presence of counter ions in the case of chemical or electrochemical doping. The localized states of a bipolaron are located further away from the band edges compared to the states of a polaron. The structures of a positive polaron and bipolaron are illustrated in Figure 2.4 together with their associated energy levels.

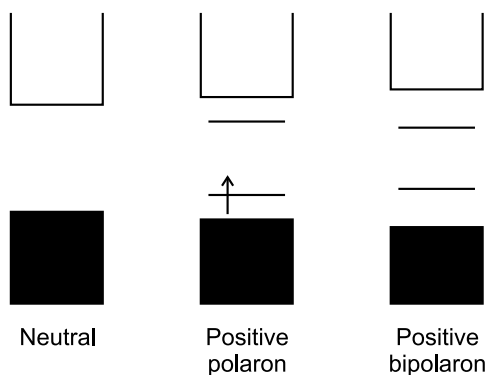
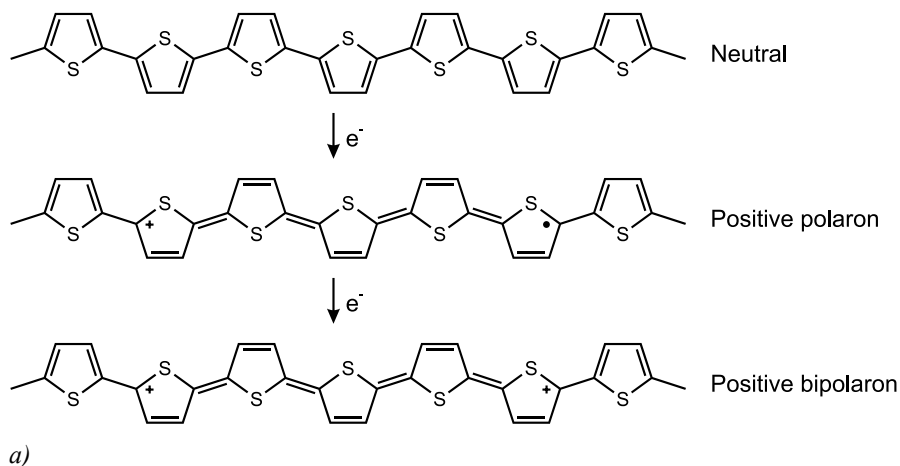


Figure 2.4. a) The structures of a neutral polymer chain, a positive polaron and a positive bipolaron, and b) their associated energy levels.

Due to weak π overlap between neighboring polymer chains, charge carriers, in the form of polarons and/or bipolarons, tend to be delocalized on individual polymer chains [29]. A charge carrier on a specific polymer chain is transported along that chain as a package that alters the positions of the single and double bonds as it moves along the polymer backbone. This type of transport along specific polymer chains alone will however not yield conduction through an entire polymer sample since the polymer chains are of finite length and usually are disordered and contain defects. Conduction through an entire polymer sample is achieved via additional transport, in the form of hopping, of charge carriers between different polymer chains. This latter mechanism, hopping of charge carriers between polymer chains, limits the electronic charge transport.

2.2. Carbon nanotubes

2.2.1. Molecular structure

Graphene is a flat monolayer of carbon atoms that are packed into a two-dimensional honeycomb lattice [30]. Just like the backbone carbon atoms in semiconducting polymers, the carbon atoms in graphene are sp^2 hybridized. Thus, for each carbon atom three of the four valence electrons are described with hybrid orbitals. These hybrid orbitals form a planar structure with an angle of 120° between the hybrid orbitals. Each hybrid orbital forms a σ bond to an adjacent carbon atom and when repeated throughout a plane, the σ bonds that are formed between the sp^2 hybridized carbon atoms create an atom-thick sheet of hexagonal rings, see Figure 2.5. The σ bonding creates a robust lattice structure [31]. The fourth valence electron, not involved in the sp^2 hybridization, of each carbon atom is described with a $2p$ atomic orbital, which is oriented perpendicular to the planar structure defined by the hybrid orbitals. The $2p$ atomic orbitals of neighboring carbon atoms can overlap and form π bonds, which result in the formation of a filled π band (valence band) and an empty π^* band (conduction band). It turns out that the conduction and valence bands touches at certain points in the graphene Brillouin zone [32-34]. This renders graphene a zero-gap semiconducting material.

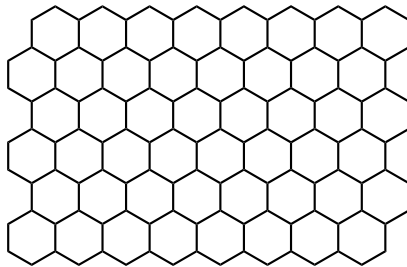


Figure 2.5. The hexagonal structure of graphene, a flat monolayer of carbon atoms, formed by the hybrid orbitals. The $2p$ atomic orbitals, not included here, are oriented perpendicular to this structure.

Here, graphene represents the basic building block for carbon nanotubes (CNTs). A single-walled CNT [35, 36] can be *considered* as a single sheet of graphene that is rolled into a seamless cylindrical tube, see Figure 2.6. CNTs can also exist in a multi-walled configuration [37], not considered here, in which several concentric tubes share a common center axis. Thus, along the walls of the cylindrical structure the carbon atoms form a hexagonal network; but the ends of the cylinder are either open or capped with a fullerene

structure (including pentagons) [38, 39]. The diameter of a single-walled CNT is 1-2 nm while its length normally exceeds 10 μm [38, 40] (CNTs that are on the order of centimeters long has been reported [41]). This gives CNTs a very large aspect ratio and they can be considered as one-dimensional electronic systems.

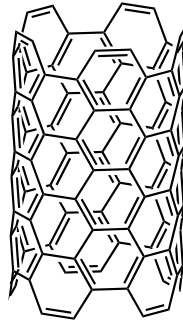


Figure 2.6. Segment of a single-walled carbon nanotube. Note the helical arrangement of hexagonal rings along the tube.

The electronic structure of CNTs is somewhat related to that of graphene but dependent on the direction, relative to its hexagonal structure, about which the graphene sheet is “rolled” into a cylinder. It has been demonstrated, both theoretically [42] and experimentally [43, 44], that CNTs can be either one-dimensional metals, which are stable against a Peierls distortion [42], or one-dimensional semiconductors depending on the helicity of the hexagonal rings along the cylinder and the nanotube diameter. Further, the energy gap of semiconducting CNTs is inversely proportional to the nanotube diameter [43, 44].

2.2.2. Carbon nanotube networks

A network of single-walled CNTs, a single-walled CNT film, contains a mixture of metallic and semiconducting CNTs [45]. Approximately one third of the nanotubes are metallic and two thirds are semiconducting. The density of nanotubes in a thin network of CNTs influences the electrical properties of the network drastically [46]. If the CNT network is sufficiently dense, individual metallic CNTs can form uninterrupted conducting pathways. Such CNT networks are metallic and reveal attractive mechanical and optical properties. They can, for instance, be utilized as transparent and flexible conductors in various applications [47, 48]. In a less dense CNT network, metallic pathways are interrupted and connected with semiconducting pathways [46]. This CNT network is semiconducting and can be used as the active material in transistors [49]. Micrometer-thick networks of CNTs have high electrical

conductivity and a nanoporous structure [50]. Their porous structure is associated with a high specific surface area (surface area per mass of the network; up to 500 m²/g [51]). Such high-surface area networks are attractive as electrodes for supercapacitors (Chapter 5) in which the capacitance value is proportional to the surface area of the electrodes.

2.3. Polymer-based electrolytes

Chemical compounds that are dissociated into free ions are called electrolytes. An electrolyte is an ionic conductor which may be in the form of a solution, a liquid or a solid [52]. Electrolyte solutions, consisting of a solute dissolved in a liquid solvent, are commonly suitable for electrochemical experiments. In such experiments, the choice of solvent is important since each solvent is associated with a stable potential window. However, from a practical point of view, ionically solid materials are often preferred instead of liquid materials in devices [53]. Primarily to avoid leakage-related problems and to allow for production of miniaturized structures with simple fabrication techniques. While some solid electrolyte systems are hard and brittle, which might cause contact problems at the electrolyte-electrode interfaces in devices without the use of liquid electrodes, the mechanical properties of polymer-based electrolytes allows for all-solid-state devices.

2.3.1. Polymer electrolytes

A polymer electrolyte, in its original sense, is referred to as a (liquid) solvent-free system in which an ionically conducting phase is created by dissolving salts in a high-molecular weight polar polymer matrix [53]. For such dry polymer electrolytes, the solvent is the polymer itself. Both the positively (cations) and negatively (anions) charged ions can be mobile. Commonly, solvent-free polymer electrolytes are based on high-molecular weight poly(ethylene oxide) (PEO, molecular structure in Figure 2.7a). PEO-based electrolytes have commonly a high degree of crystallinity at ambient temperatures. This results in a poor ionic conductivity in these electrolytes. One approach to achieve higher ionic conductivities relates to introducing small polar molecules into the polymer electrolyte. Such so-called gel electrolytes are commonly referred to as polymer electrolytes but are created by dissolving a salt in a polar solvent and adding a polymer network to give the electrolyte mechanical stability.

2.3.2. Polyelectrolytes

Polyelectrolytes are materials that have a polymeric backbone with electrolytic groups covalently attached to it [53]. The electrolytic groups can be salts, acids and bases. Commonly, polyelectrolytes dissociate into ions in polar solvents. This results in charged

polymer chains and oppositely charged counter ions. Depending on the chemical nature of the polyelectrolyte, the polymer chains become negatively or positively charged. A polymer chain that is negatively (positively) charged is called a polyanion (polycation). Since the polymer chains are immobile in the solid state, only one type of mobile ion exists in polyelectrolyte films. This is advantageous; it makes, for instance, the interpretation of conductivity measurements much simpler than for polymer electrolytes. The molecular structures of a polyanion- and a polycation-based polyelectrolyte are given in Figure 2.7b and c, respectively.

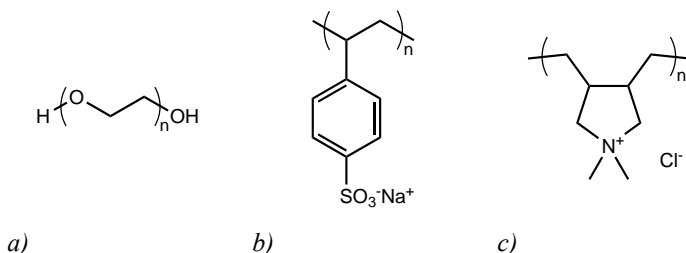


Figure 2.7. Molecular structures of a) poly(ethylene oxide) (PEO), b) poly(styrene sulfonate) with sodium as the mobile charge carrier (PSS:Na, polyanion-based polyelectrolyte), and c) poly(diallyldimethylammonium chloride) (polycation-based polyelectrolyte).

2.3.3. Ionic charge transport

The ionic transport mechanisms are dependent on the type of electrolyte. The major differences between the ionic motion in a polymer electrolyte and in a polyelectrolyte or a gel electrolyte are the molecular weight of the “solvent” and the interaction between the ions and the medium. In polymer electrolytes, the polymer matrix considered as the solvent for the ions have a high molecular weight. The polymer matrix, the solvent, is thus immobile and unable to participate in long-range motion. The ionic motion in polymer electrolytes takes place via sites that are created and destroyed on a continuous basis as a result of segmental motion of the polymer chains [53]. In a polyelectrolyte or in a gel electrolyte, on the other hand, low-molecular weight solvents form a solvation shell around the ions. In these systems, the ions can move together with the solvent molecules belonging to the solvation shells. Since they are transported through the solvent they experience a frictional force related to the viscosity of the solvent, the size of the polymer network and the size of the solvated ions.

3. Impedance spectroscopy

3.1. Basic principles

Impedance spectroscopy is a powerful tool for the characterization of several of the electrical and electrochemical properties of a material and its interfaces with electrodes [54]. The material to be characterized can be in the solid or liquid state; and the method can investigate ionic, semiconducting or insulating (dielectric) properties. The sample is commonly situated inside a small measurement cell with metal electrodes at the ends, forming a sandwiched structure as illustrated in Figure 3.1. In the standard impedance spectroscopy approach, the impedance is measured by applying an alternating voltage with a specific frequency (f) to the two electrodes of the measurement cell and measuring the amplitude and phase shift of the resulting current at this frequency. This procedure is repeated for a number of frequencies within a specific frequency range, allowing the impedance to be measured as a function of frequency.

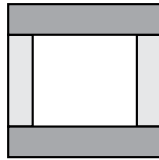


Figure 3.1. Cross-sectional illustration of a measurement cell. The material under test is located in the white center area, the top and bottom layer corresponds to the metal electrodes while the light grey walls hold the (liquid) material within the cell.

The frequency-dependent complex impedance (Z) is defined in Equation 3.1 where ω is the angular frequency ($\omega = 2\pi f$), V is a complex voltage and I is a complex current.

$$Z(\omega) = \frac{V}{I} \quad (3.1)$$

Further, this impedance can be expressed as the sum of a frequency-dependent real part (Z_{Re}) and a frequency-dependent imaginary part (Z_{Im}) according to Equation 3.2 where j represents the imaginary number. The phase angle (θ) of the complex impedance is given in Equation 3.3.

$$Z(\omega) = Z_{\text{Re}} + jZ_{\text{Im}} \quad (3.2)$$

$$\theta(\omega) = \tan^{-1}\left(\frac{Z_{\text{Im}}}{Z_{\text{Re}}}\right) \quad (3.3)$$

With experimental data of the total complex impedance of a specific system in hand, either an electrical equivalent circuit or a mathematical model based on a physical theory is needed. Next, the experimental impedance data can be compared, or fitted, to the impedance expression of either the equivalent circuit or the mathematical model. It is only after that the information and parameters related to the electrical properties of the full system can be estimated. The parameters derived from an impedance spectroscopy measurement are generally grouped into two main categories:

1. Parameters that only are related to the material itself, examples are the dielectric constant and the conductivity of a material.
2. Parameters that are related to an electrode-material interface, examples are the capacitance of an interface region and parameters related to reactions at an interface.

Most of the electrical equivalent circuits contain ideal resistors and capacitors, while inductors rarely are included; the impedance expressions and phase angles of these circuit elements are summarized in Table 3.1. Usually, the resistors are used to describe irreversible processes such as interfacial charge transfer and charge transport, while the capacitors are used to describe reversible processes such as charge polarization or storage. The impedance response of four different equivalent circuits based on ideal resistors and capacitors are given in the form of Nyquist plots ($-Z_{\text{Im}}$ versus Z_{Re}) in Figure 3.2. Note that each point in a Nyquist plot corresponds to the impedance values at a specific frequency. The direction of the frequency is indicated with an arrow in the plots. The four different equivalent circuits in Figure 3.2 can,

for instance, be used to describe: a) an electric double layer, b) an electric double layer together with the resistance of an electrolyte, c) an electrochemical interface of a metal and an electrolyte where the resistor describes interfacial charge transfer and the capacitor describes the double layer at the interface, and d) an electrochemical interface as described in c) but with an additional resistor to account for the resistance of the electrolyte bulk. Thus, one way to obtain information or hints about a possible equivalent circuit of a specific system is to plot the experimental impedance data in a Nyquist plot and analyze its shape.

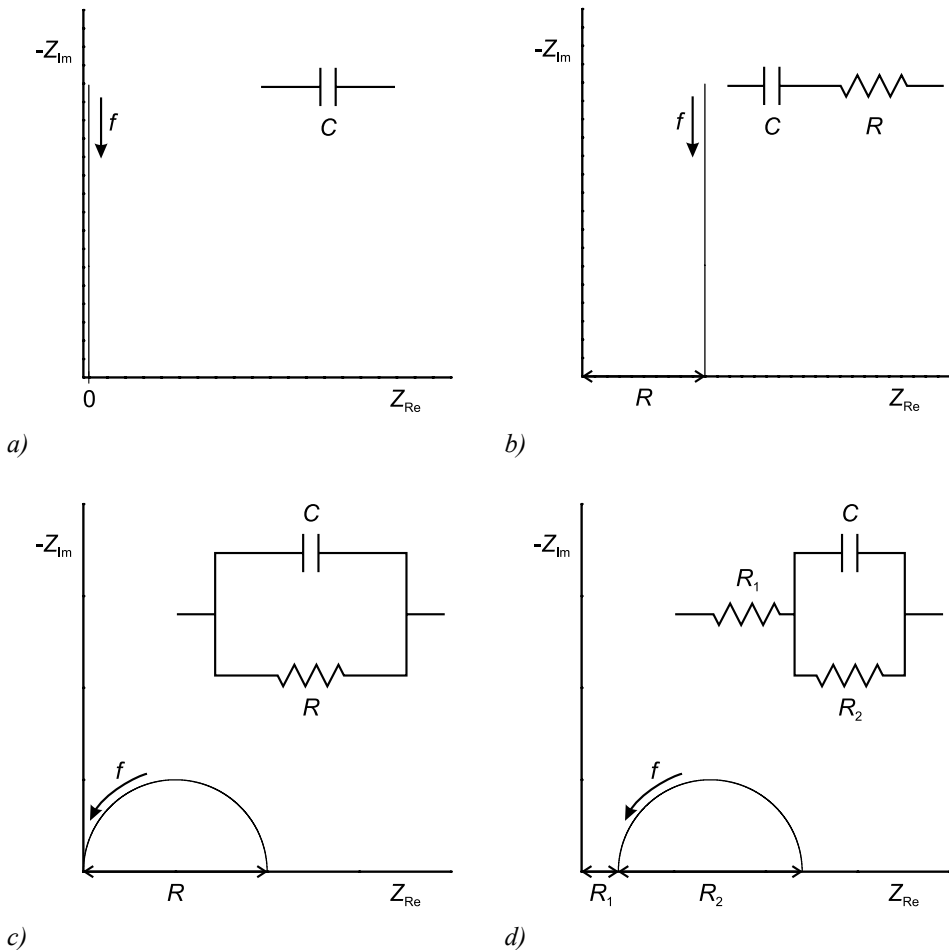


Figure 3.2. Four different equivalent circuits and their impedance responses presented as Nyquist plots. Note the direction of the frequency. From the plots, the values of the resistors can easily be obtained as indicated. The value of the capacitors can be calculated from the imaginary part of the impedances using the relation given in Table 3.1.

Circuit element	Impedance (Ω)	Phase angle ($^\circ$)
Resistor	$Z_R = R$	0
Capacitor	$Z_C = 1/(j\omega C)$	-90
Inductor	$Z_L = j\omega L$	90
Warburg impedance [55]	$Z_W = A/(j\omega)^{0.5}$	-45
Constant phase element [54]	$Z_{CPE} = 1/[Q_\alpha(j\omega)^\alpha]$	-90α ($0 \leq \alpha \leq 1$)

Table 3.1. The impedance expressions and the phase angles of the ideal circuit elements (resistor, capacitor and inductor) and the two most commonly used distributed circuit elements (the Warburg impedance and the constant phase element).

However, impedance data of real world systems cannot always be described with equivalent circuits comprising only ideal circuit elements. This originates from the assumption that the time it takes for an electronic signal to travel between the circuit elements in a circuit is negligible. That is equivalent to considering the entire circuit to be located at a single point in space. However, in reality all systems are extended over a finite region of space, they are said to be distributed in space, rather than being localized at a single point. In addition, their microscopic properties might be distributed as well. Often, experimental impedance data exhibit a distributed behavior. In those cases, so-called distributed circuit elements need to be incorporated into the equivalent circuit to be able to approximate the experimental impedance with an equivalent circuit. The impedance of a distributed circuit element cannot be expressed exactly with a finite number of ideal circuit elements. Two of the most frequently used distributed circuit elements are the Warburg impedance and the constant phase element (CPE).

First; the Warburg impedance and its related phase angle are given in Table 3.1 where A is a positive constant [55]. This impedance element is related to mass transfer resistance and is specifically derived for (one-dimensional) diffusion of a particle [56]. From experimental impedance data, it is possible to estimate diffusion coefficients via the constant A . The Warburg impedance is frequently used within electrochemistry. Second; the CPE is an empirical impedance function with its impedance and phase angle given in Table 3.1 [54]. Q_α is a positive constant with its dimension altering with α , where α is a constant in the range $0 \leq \alpha \leq 1$. Note that: $\alpha = 0$ reveals the case of an ideal resistor with $R = Q_\alpha^{-1}$, $\alpha = 0.5$ gives the Warburg impedance with the constant $A = Q_\alpha^{-1}$, and that $\alpha = 1$ corresponds to the case of an

ideal capacitor with $C = Q_{\alpha}$. CPEs are, for instance, frequently used in equivalent circuits to describe impedance data of solid and liquid electrolytes. In the literature, numerous different equivalent circuit models exist [54, 57]. Below, a few but general equivalent circuits are presented and described briefly.

3.2. Common equivalent circuits

3.2.1. The Debye equivalent circuit

The nominal time scale for which molecular reorientation or ion jumps can occur is called the relaxation time (τ) [58]. The basic model of dielectric relaxation is described with the Debye equivalent circuit [54, 59], see Figure 3.3a. The impedance response of this circuit is presented in a Nyquist plot in Figure 3.3b. This model is derived for materials with an absence of conductivity under the assumption of a single relaxation time. In the equivalent circuit, C_1 represents polarization established even at high frequencies of the applied field, while C_2 represents polarization established at low frequencies only. R represents the mechanism that acts to prevent the low-frequency polarization from being established at higher frequencies. The single relaxation time in this model is given by $\tau = RC_2$. However, dielectric relaxation in many dielectric materials does not follow the Debye model with accuracy.

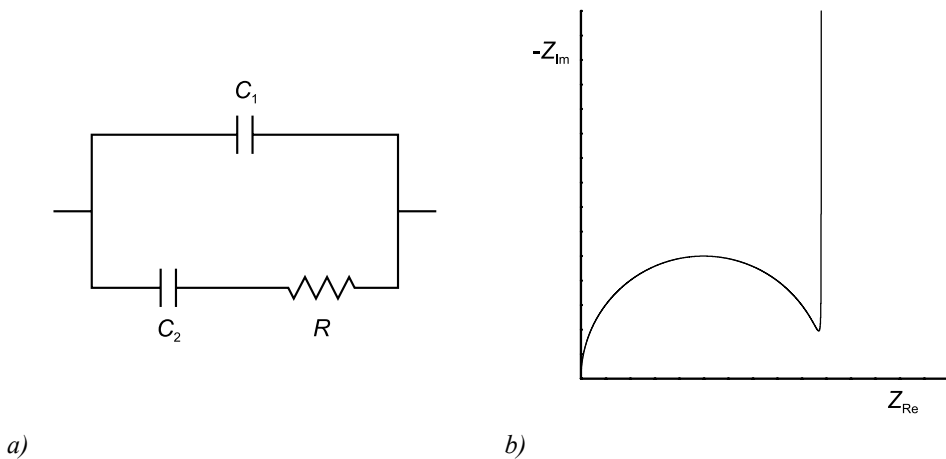


Figure 3.3. a) The Debye equivalent circuit, and b) its impedance response presented in a Nyquist plot.

3.2.2. The Cole-Cole equivalent circuit

The Cole-Cole model [59], described with the equivalent circuit in Figure 3.4a, of dielectric relaxation is derived for materials with an absence of conductivity and with a distribution of relaxation times [54]. In this model, this distribution is symmetric around a central relaxation time. The interpretation of the circuit elements in this equivalent circuit is identical to that of the Debye equivalent circuit with one exception; the mechanism that acts to prevent the low-frequency polarization from being established at higher frequencies is represented by *CPE* in this circuit. Note that the Cole-Cole equivalent circuit will collapse into the Debye equivalent circuit if $\alpha = 0$. Thus, the distribution of relaxation times is related to the CPE and specifically to α ; a low (high) value of α corresponds to a narrow (wide) distribution. In Figure 3.4b, the impedance response of the Cole-Cole circuit is given for various values of α .

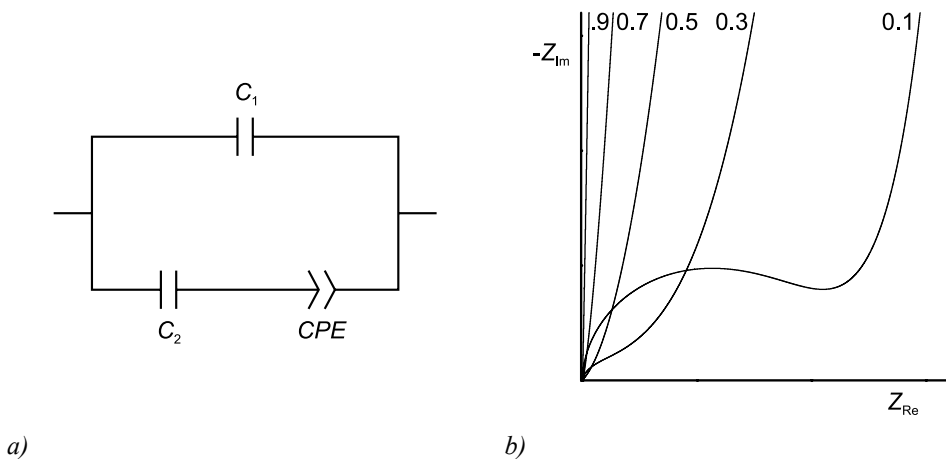


Figure 3.4. a) The Cole-Cole equivalent circuit, and b) its impedance response, for various values of α , presented in a Nyquist plot.

3.2.3. The Randles equivalent circuit

A frequently used equivalent circuit for electrochemical cells is the Randles equivalent circuit [52, 56]. This equivalent circuit is given in Figure 3.5a together with an illustration of an electrochemical half-cell (an electrode and an electrolyte). In this circuit, R_{CT} and C_{DL} are related to the electrolyte-electrode interface. R_{CT} represents interfacial charge transfer and C_{DL} represents the double layer formed at the interface. Further, the Warburg impedance (Z_W) is related to the diffusion layer. A slope of 45° at low frequencies of the impedance curve in the

Nyquist plot (Fig. 3.5b) is a characteristic of diffusion limitation at these frequencies. The last circuit element in this equivalent circuit, R_E , represents the electrolyte resistance.

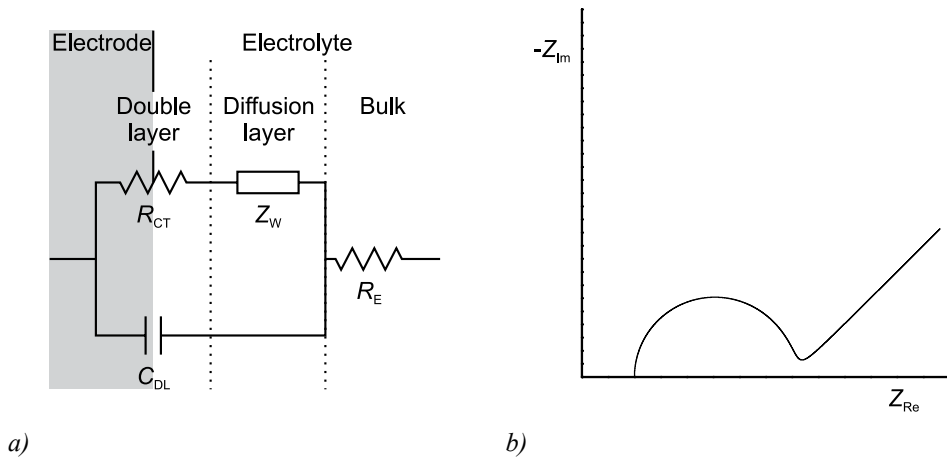


Figure 3.5. a) The Randles equivalent circuit together with an illustration of an electrochemical half-cell, and b) the impedance response of this circuit presented in a Nyquist plot. See text for details.

4. Polarization in capacitor structures

A capacitor consists of two electrical conductors separated from each other by an insulating material. The capacitance (C) between these two conductors is defined in Equation 4.1, where Q ($+Q$ on the positively biased side and $-Q$ on the grounded side) is the charge stored at or carried by each conductor and V is the potential difference between the two conductors.

$$C = \frac{Q}{V} \quad (4.1)$$

The charge polarization mechanisms and characteristics in capacitors are dependent on the character of the insulating material and the frequency of the applied field. Here, the polarization is described for capacitors with an organic dielectric material, and with an electrolyte, respectively, as the insulating material.

4.1. Polarization in capacitors based on dielectric materials

A dielectric material is a material that has no free charges that can move through the material under the influence of an electric field [60]. Since all electrons in a dielectric material are bound, the only possible motion of charges upon exposure to an electric field is just very small displacements, in opposite directions, of positive and negative charges. A dielectric material in which such charge displacement has occurred is said to be polarized and its molecules are said to have induced dipole moments. The induced dipole moments are temporary and disappear when the electric field is removed. In addition, an electric field can also orient permanent dipole moments in the material. Here, focus is on the orientation of permanent dipole moments in organic polymers. A solid-state material, such as an insulating polymer, sandwiched between two metal electrodes, forming a parallel-plate capacitor structure, is illustrated in Figure 4.1a.

In a polymer, polar covalent bonds give rise to permanent dipole moments. These permanent dipole moments experience a torque that tends to align them with an applied electric field. In the solid state, the polar bonds tend to align, or rotate, with the electric field. This results in an equilibrium polarization with a net alignment of the permanent dipole moments with the applied field, idealized illustration given in Figure 4.1b. Additionally, the whole molecules themselves are capable to align with the electric field in the liquid state. The applied voltage between the metal electrodes results in a constant electric field (and linear potential profile) across the dielectric material. As the polarity of the applied voltage is reversed, the permanent dipole moments align with the new direction of the electric field (Fig. 4.1c). The polarity of the applied voltage can be modified with an ac voltage. Above a specific frequency of the applied ac voltage, the electric field changes direction faster than the permanent dipole moments can realign. As a result, the permanent dipole moments will not contribute to the polarization at these frequencies. This specific frequency is dependent on the strength of the molecular interaction within the material. It can be very high for a molecule in a fluid, and is typically much lower in a solid [61, 62]. When the applied voltage is disconnected, the permanent dipole moments become randomly oriented and the polarization is lost (Fig. 4.1a).

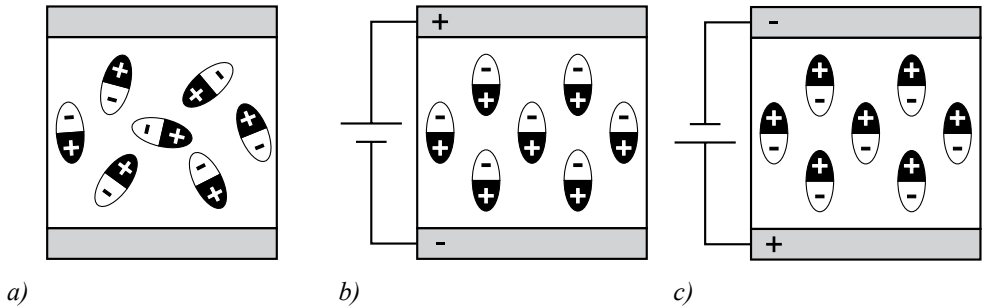


Figure 4.1. Idealized illustration of the polarization, due to the orientation of permanent dipole moments, in a capacitor (a dielectric polymer sandwiched between two metal electrodes). a) With no voltage applied, the permanent dipole moments are randomly oriented, b) with a voltage applied, the dipole moments align with the electric field, and c) when the polarity of the voltage is reversed, the dipole moments align with the new direction of the electric field.

The capacitance of a parallel-plate capacitor with a dielectric material as the insulating layer is given in Equation 4.2, where ϵ_0 is the permittivity of free space, κ is the relative dielectric constant of the dielectric material, A is the capacitor plate area and d is the thickness of the

dielectric material. A material with a large relative dielectric constant corresponds to a material that is highly polarizable.

$$C = \frac{\epsilon_0 \kappa A}{d} \quad (4.2)$$

4.2. Polarization in capacitors based on electrolytes

In contrast to dielectric materials, electrolytes have free (ionic) charges that can move in an electric field. An illustration of a parallel-plate capacitor consisting of an electronically insulating but ion-conducting electrolyte sandwiched between two metal electrodes is given in Figure 4.2a. When a voltage is applied to the capacitor, redistribution of ions takes place in the electrolyte. Positively charged ions (cations) migrate towards the negatively charged electrode while negatively charged ions (anions) migrate towards the positively charged electrode (Fig. 4.2b). At the electrolyte-electrode interfaces so-called electric double layers are formed (Fig. 4.2c).

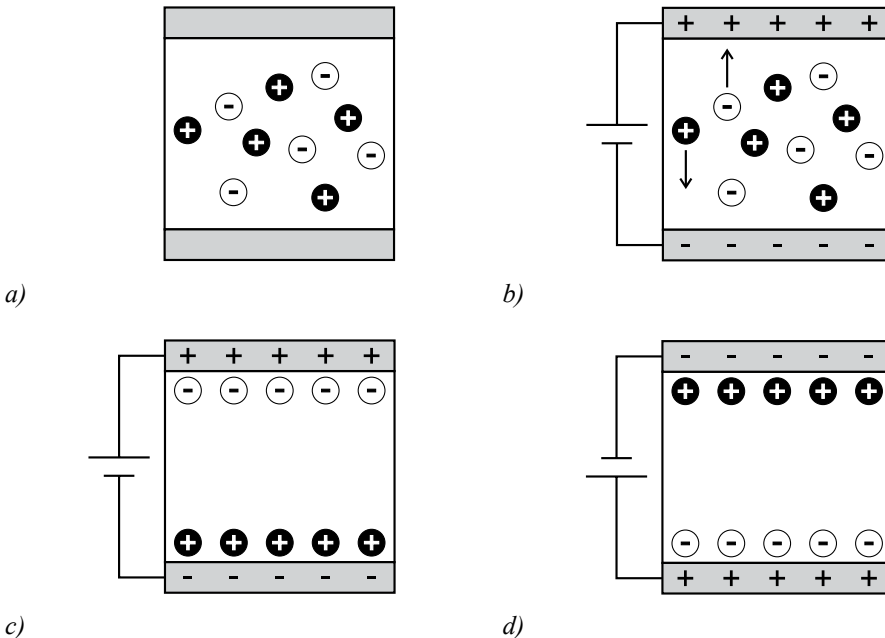


Figure 4.2. Idealized illustration of the polarization in a capacitor with an electrolyte sandwiched between the two metal electrodes. a) With no voltage applied, the ions in the electrolyte are randomly distributed. When a voltage is applied, b) ions migrate towards the oppositely charged electrode and c) form electric double layers at the interfaces. In d), the polarity of the applied voltage is reversed.

Although electric double layers are formed at both interfaces, the discussion below will treat only one of them. The charge in the metal electrode (negative or positive dependent on the polarity of the applied voltage) is located within a very thin sheet ($< 0.1 \text{ \AA}$) along the surface of the metal [56]. The charge on the electrolyte side is made up of a surplus of ions (cations or anions dependent on the charge on the metal electrode) in the vicinity of the metal electrode surface. This ensemble of positive and negative charges, together with oriented dipole moments, at the electrolyte-metal electrode interface is called an electric double layer. Commonly, the structure of an electric double layer is described with the so-called Gouy-Chapman-Stern (GCS) model [56, 61]. In the GCS model the electrolyte side consists of different layers, see illustration in Figure 4.3. Closest to the metal electrode there is a layer that contains solvent molecules; this layer is called the compact layer or the Helmholtz layer. Next, a layer is formed consisting of solvated ions located at a distance x away from the metal electrode, that interacts with the charged metal electrode via electrostatic forces. The potential profile from the metal electrode to x is linear; this region is represented by a capacitor C_H . The next layer is a diffuse layer that extends from x into the bulk of the electrolyte. In this layer, closest to the metal electrode there is an excess of ions that are oppositely charged compared to the metal electrode. The potential profile in this layer decreases non-linearly towards the bulk of the electrolyte; this layer is represented by a capacitor C_D . The capacitance of the entire double layer, represented by C_H in series with C_D , is typically on the order of tens of $\mu\text{F}/\text{cm}^2$ [56]. Note that the electric field will be confined to the double layers. To compare with a dielectric capacitor, the capacitance of a 100 \AA thin SiO_2 layer is $\sim 0.35 \mu\text{F}/\text{cm}^2$ ($\kappa = 3.9$).

When the polarity of the voltage applied to the capacitor, described in Figure 4.2, is reversed cations migrate towards the now negatively charged electrode while anions migrate towards the positively addressed electrode. Again, electric double layers are formed at the interfaces (Fig. 4.2d). An ac voltage can be used to cycle the polarity of the applied voltage. Now, if the frequency of the applied ac voltage is increased, a frequency is reached where the ions do not have enough time to form electric double layers. Above this frequency the ions migrate back and forth when the direction of the electric field is changed, they oscillate. When the applied voltage is disconnected, the ions become randomly distributed and the polarization is lost (Fig. 4.2a).

As with ordinary electrolytes, electric double layers will form at the interfaces when a polyelectrolyte is used as the insulating material sandwiched between the metal electrodes in Figure 4.2. However, since one of the charged species in a solid polyelectrolyte is practically immobile (polyanion or polycation dependent on the polyelectrolyte) the formation of one of the electric double layers will be different. Positively (negatively) charged mobile ions will migrate towards the negatively (positively) charged electrode and form an electric double layer at that interface, while the double layer at the other interface is formed from immobile polyanions (polycations) located close to the positively (negatively) charged electrode. At high frequencies, the mobile ions oscillate along the charged polymer chains.

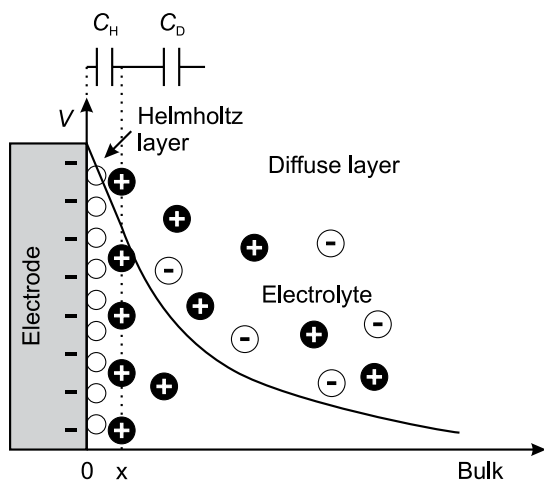


Figure 4.3. Illustration of the Gouy-Chapman-Stern model of the structure of an electric double layer. The empty circles represent solvent molecules and the black (white) circles with a '+' ('-') sign represent solvated cations (anions). See text for details.

5. Devices

5.1. Polymer-based humidity sensors

5.1.1. Resistive- and capacitive-type sensors

Humidity sensors with a mode of operation that is based on a change of the electrical impedance are commonly divided into two different groups; resistive- and capacitive-type sensors [63]. The resistive-type of sensors utilizes a change of the real part of the impedance of the active sensing material upon exposure to a change of ambient humidity, while the capacitive-type of sensors are associated with a change of the imaginary part of the impedance. In the most common device configurations, regarding both resistive- and capacitive-type sensors, the humidity-sensitive material is either sandwiched between two electrodes or deposited between interdigitated electrodes [64]. Among other materials, polyelectrolytes have been identified as good candidates for resistive-type humidity sensors due to their high sensitivity, quick response and low cost [65]. The molecular structure of poly(styrenesulfonic acid) (PSS:H), a commonly used material for resistive-type sensors, is given in Figure 5.1a [64]. As water is absorbed into the polyelectrolyte film the number of mobile counter-ions that are dissociated from the electrolytic groups of the polyelectrolyte, providing ionic current transport in the film, and the ionic mobility of the polyelectrolyte both change [66]. Typically, the conductivity of polyelectrolytes increases nonlinearly with humidity [67, 68].

Although solid polyelectrolytes have been reported as a suitable class of materials for capacitive-type sensors as well [69], the most common choice of materials for capacitive-type sensors are various insulating polymer films [64]. In Figure 5.1b, the molecular structure is given for poly(methyl methacrylate) (PMMA), an insulator material commonly used in capacitive-type sensors [64]. Absorption of water into the dielectric polymer film causes the dielectric constant to change, thus modulating its capacitance (Eq. 4.2). Due to the high dielectric constant of the absorbed water, the capacitance of these materials increases with

humidity. Capacitive-type sensors are in general more expensive as compared to resistive-type sensors, but they reveal more attractive characteristics on the other hand. Normally, they can be operated over a wider humidity range and exhibits a linear response with humidity, making the circuitry for interpretation of the humidity-readout less complex [68].

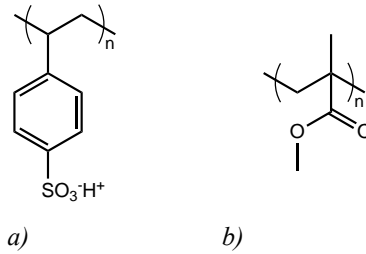


Figure 5.1. Molecular structures of a) poly(styrenesulfonic acid) (PSS:H), a commonly used polyelectrolyte for resistive-type humidity sensors, and b) poly(methyl methacrylate) (PMMA), a commonly used polymer for capacitive-type humidity sensors.

5.1.2. Wireless readout and sensing of passive resonance sensor circuits

A resonance circuit is an electrical circuit having an inductive and capacitive part. The simplest possible resonance circuit contains one inductor (L) and one capacitor (C) and is often referred to as a LC circuit. Such LC circuits can be configured in either a serial or parallel configuration (Fig. 5.2a and b). The total impedance of the serial (Z_{Serial}) and parallel (Z_{Parallel}) configurations are given by Equations 5.1-5.2.

$$Z_{\text{Serial}} = Z_L + Z_C = j\omega L - j\frac{1}{\omega C} = j\left(\omega L - \frac{1}{\omega C}\right) \quad (5.1)$$

$$Z_{\text{Parallel}} = \frac{Z_L Z_C}{Z_L + Z_C} = \frac{j\omega L \frac{-j}{\omega C}}{j\omega L - \frac{j}{\omega C}} = \frac{\frac{L}{C}}{j\left(\omega L - \frac{1}{\omega C}\right)} \quad (5.2)$$

At a specific frequency, called the resonance frequency (f_0), a large peak will be observed in the frequency response of the transfer function ($|V_{\text{Out}}/V_{\text{In}}|$ versus f , Fig. 5.2c). For the serial configuration, this peak will be observed at the frequency where the total impedance equals zero (Eq. 5.1), meaning that the LC circuit will act as an electrical short at f_0 . The resonance frequency of the parallel configuration will be observed at the frequency where the total

impedance goes to infinity, in other words where the denominator equals zero (Eq. 5.2), meaning that the LC circuit will act as an open circuit at f_0 . The resonance frequency of a LC circuit, in serial or parallel configuration, is given by Equation 5.3. Note that additional reactive circuit elements added to a resonance circuit result in complex analytical expressions of its total impedance and resonance frequency.

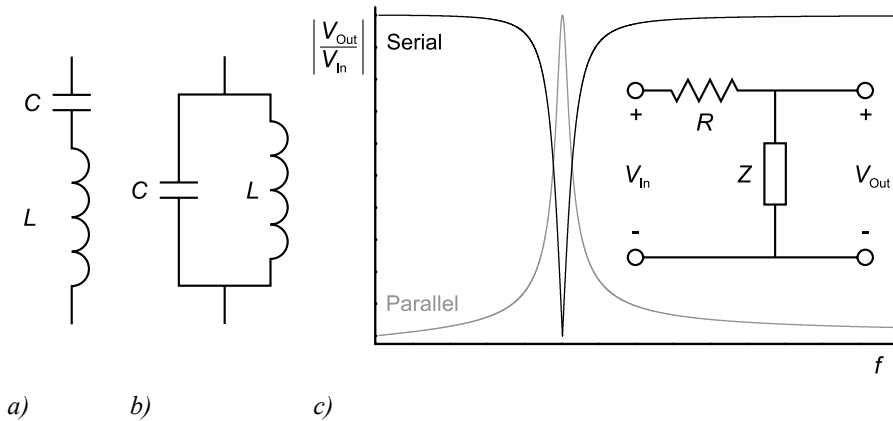


Figure 5.2. a) Serial and b) parallel configurations of LC circuits. c) The transfer function of each LC circuit versus the frequency, Z corresponds to the circuits in a) and b). The frequencies at the peaks correspond to the resonance frequencies.

$$f_0 = \frac{1}{2\pi\sqrt{LC}} \quad (5.3)$$

Now consider a circuit consisting of an ac voltage source connected to an inductor, called the primary side, separated from an unpowered LC circuit, called the secondary side, as illustrated in Figure 5.3a. The primary and secondary sides are mutually coupled within a certain physical distance. The current (I_P) through the inductor (L_P) of the primary side creates an alternating magnetic field that induces an alternating voltage ($V_{S, \text{Ind}}$) across the inductor (L_S) of the secondary side. $V_{S, \text{Ind}}$ drives an alternating current (I_S) through the secondary side. The current through L_S creates in turn an alternating magnetic field that induces an alternating voltage ($V_{P, \text{Ind}}$) across L_P , driving an alternating current through the primary side. The resulting circuit scheme of this mutual coupling is given in Figure 5.3b.

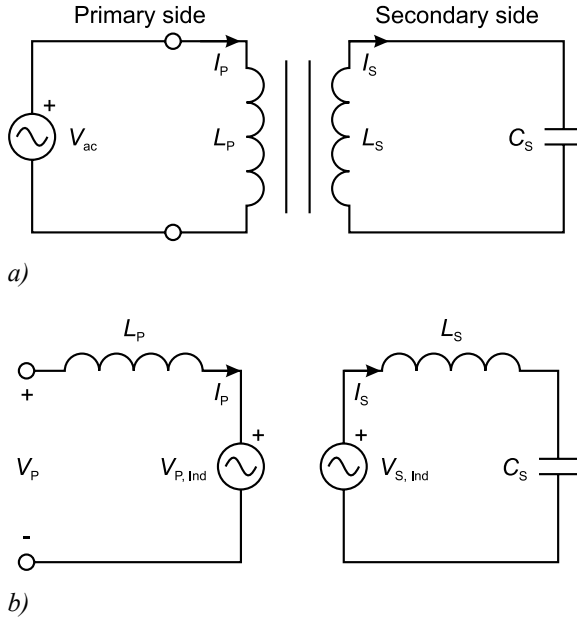


Figure 5.3. a) An ac voltage source connected to an inductor, forming the primary side, mutually coupled to a LC circuit that forms the secondary side. The circuits in b) represent the equivalent circuits of the mutual coupling. See text for details.

If sinusoidal voltages and currents are assumed, the expressions for $V_{S, Ind}$ and $V_{P, Ind}$ are given in Equations 5.4-5.5, where M represents the mutual inductance between the primary and secondary sides.

$$V_{S, Ind} = j\omega MI_p \quad (5.4)$$

$$V_{P, Ind} = -j\omega MI_s \quad (5.5)$$

By applying Kirchhoff's voltage law on the primary and secondary sides, the following equations are obtained from the primary (Eq. 5.6) and secondary (Eq. 5.7) sides:

$$V_p = j\omega L_p I_p - j\omega MI_s \quad (5.6)$$

$$j\omega MI_p = I_s \left(j\omega L - \frac{j}{\omega C} \right) = I_s Z_s \quad (5.7)$$

where Z_S corresponds to the total impedance of the secondary side. Substitution of I_S (Eq. 5.7) into Equation 5.6 gives the total impedance of the primary side (Z_P) (Eq. 5.8). As shown in Equation 5.8, the total impedance of the secondary side is reflected to the primary side. The reflected impedance (Z_R) is given in Equation 5.9.

$$Z_P = \frac{V_P}{I_P} = j\omega L_P + \frac{\omega^2 M^2}{Z_S} \quad (5.8)$$

$$Z_R = \frac{\omega^2 M^2}{Z_S} \quad (5.9)$$

The impedance reflection implies that the impedance of the secondary side can be readout from the primary side without the need of a power source on the secondary side since all energy needed is induced from the primary side. Thus, passive and wireless readout of the resonance frequency of a LC circuit is possible. This concept has been utilized by others to form LC circuits built up from capacitive-type humidity sensors together with an inductor, enabling wireless readout of the humidity level (Eq. 5.3) [70-72].

5.2. Organic field-effect transistors

5.2.1. Device operation

The field-effect transistor (FET) is a three-electrode device (source, drain and gate) that is built up from electrically conducting, semiconducting and insulating materials. In an organic FET (OFET) the semiconducting layer is an organic material, for instance a semiconducting polymer. A schematic illustration of one electrode configuration is given in Figure 5.4, where L defines the channel length and W is the channel width.

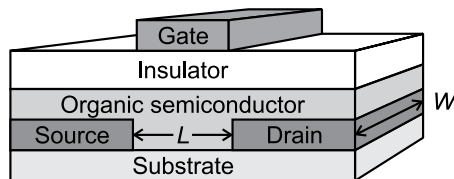


Figure 5.4. Schematic illustration of an organic field-effect transistor with channel length L and channel width W .

In FETs, the current through the transistor channel is controlled with a voltage applied to the gate electrode. OFETs operate in the accumulation mode in which an increase in gate voltage is associated with an enhanced conductivity along the transistor channel [73]. The gate electrode together with the gate-insulating layer and the organic semiconductor form a capacitor-like structure as illustrated in Figure 5.5a. Consequently, when a voltage is applied to the gate electrode, the gate insulator becomes polarized and charges are injected into the organic semiconductor from the source electrode, thus establishing the transistor channel, to charge the lower semiconducting capacitor plate. For many OFETs, so-called p -channel operation is most convenient [74]. For those transistors a negative voltage is applied to the gate electrode, followed by accumulation of positive (p) charge carriers in the transistor channel. A voltage applied to the drain electrode drives the output current of the transistor. A change in gate voltage results in modulation of the charge carrier density within the transistor channel and thus a modulation of the output current of the transistor. All of the accumulated charge carriers in the transistor channel are however not mobile, some of them are trapped in localized states at the semiconductor-insulator interface. When a voltage is applied to the gate electrode, those traps need to be filled before additional accumulated charge carriers can be transported [74]. This gives that mobile charge carriers in the transistor channel are obtained first after that the applied gate voltage (V_G) exceeds a threshold voltage (V_T). Thus, below the threshold voltage ($V_G < V_T$) the transistor is in an off mode. For higher gate voltages ($V_G > V_T$), the evolution of the drain current (I_D) with increasing drain voltage (V_D) is described as follows (Fig. 5.5b-d):

- For low values of V_D the distribution of charge carriers is almost constant along the transistor channel, see Figure 5.5b. This results in a linear increase of I_D with increasing V_D . This regime is called the linear regime and Equation 5.10 predicts the drain current ($I_{D, Lin}$) where μ is the charge carrier mobility of the semiconductor and C_i is the capacitance per unit area of the gate insulator.

$$I_{D, Lin} = \frac{W}{L} \mu C_i (V_G - V_T) V_D \quad (5.10)$$

- As V_D increases a point is reached where the charge carrier concentration in the transistor channel becomes zero close to the drain electrode (Fig. 5.5c). This point is called the pinch-off point and results in saturation of I_D ($I_D = I_{D, Sat}$ at $V_D = V_{D, Sat}$).

- As V_D is further increased ($V_D > V_{D, \text{Sat}}$) the pinch-off point moves further towards the source electrode, see Figure 5.5d. The potential at the pinch-off point ($V(x)$) remains constant ($V(x) = V_{D, \text{Sat}}$), which results in a constant potential drop between the pinch-off point and the source electrode. As a result, the effective voltage applied to the channel will equal $V_{D, \text{Sat}}$ and I_D will remain constant ($I_D = I_{D, \text{Sat}}$). This regime corresponds to the saturated regime with a saturation current given by Equation 5.11.

$$I_{D, \text{Sat}} = \frac{W}{2L} \mu C_i (V_G - V_T)^2 \quad (5.11)$$

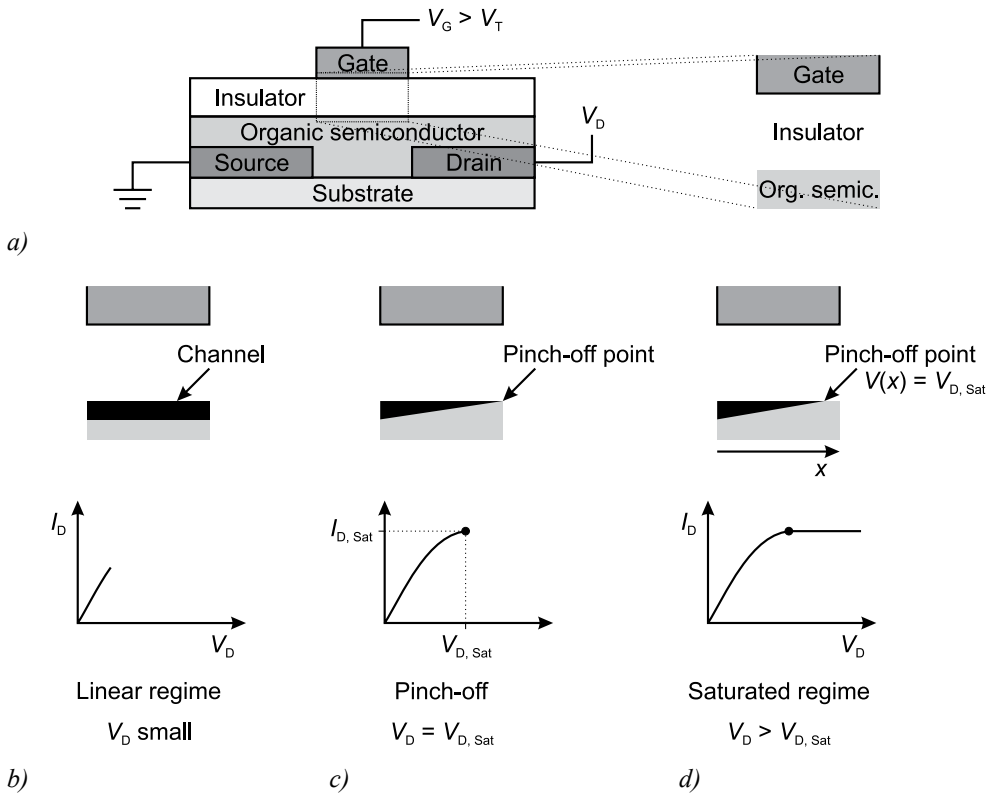


Figure 5.5. a) Schematic illustration of an organic field-effect transistor in which the capacitor-like structure, formed by the gate electrode, the insulator and the semiconductor, is zoomed-in. b-d) Illustrations of the operating regimes of the transistor with help of the zoomed-in structure in a) and corresponding current-voltage characteristics. b) The linear regime, c) pinch-off, and d) the saturated regime. See text for details.

For many electronic applications considered for OFETs, there is a demand for switching on and off at high frequencies and that these devices are capable of delivering high output currents at low driving voltages. Most often, the time response of an OFET is limited by the transit time (τ , Eq. 5.12 [75]) of the charge carriers through the transistor channel.

$$\tau \approx \frac{L^2}{\mu |V_D|} \quad (5.12)$$

From Equations 5.10-5.12 it is evident that a high charge carrier mobility of the semiconductor is essential in order to obtain high output currents and fast time response, at a given channel geometry, of OFETs. For this reason, much research has been devoted to find high-mobility organic semiconducting materials. Although the mobility is related to the nature of the semiconducting material, it is affected by several factors. It has been reported that good chain configuration (high regio-regularity) [76], a high molecular weight [77] and a high degree of crystallinity [78] of the polymer are key factors to achieve a high mobility. The degree of crystallinity depends on the deposition method and can in some cases, for solution-processed polymers, be improved by the proper choice of solvent [78].

5.2.2. Organic field-effect transistors operated at low voltages

One major drawback with OFETs is that they in general require high operational voltages, often several tens of volts [73]. This excludes OFETs in typical low-end applications where the available voltages are expected to be very low [79]. Currently, much attention is focused on lowering this operational voltage of OFETs and to simultaneously maintain as high output currents as possible. This implies that for a given charge carrier mobility of the semiconductor, the amount of accumulated charge carriers in the transistor channel should be as high as possible. At a specific gate voltage ($V_G > V_T$), without any V_D applied, the accumulated mobile charge per unit area (Q_m) in the transistor channel is related to the gate voltage via Equation 5.13.

$$Q_m = C_i(V_G - V_T) \quad (5.13)$$

Clearly, a high capacitance per unit area of the gate insulator is required for low-voltage operation of OFETs while also keeping the output current as high as possible (Eq. 5.10-5.11). The capacitance per unit area of a gate-insulating dielectric material is given in Equation 5.14,

where ϵ_0 is the permittivity of free space, κ is the relative dielectric constant and d is the thickness of the dielectric layer.

$$C_i = \frac{\epsilon_0 \kappa}{d} \quad (5.14)$$

Hence, there are two different methods to increase the capacitance per unit area of a dielectric gate insulator: (i) change to a material with a large dielectric constant (high- κ materials) [80] or (ii) decrease the film thickness of the gate insulator [81, 82].

An alternative approach in reaching low driving voltages in OFETs is to use an electrolyte as gate insulator instead of dielectric materials [83-89]. The operation of an electrolyte-gated OFET is analogous to that of an ordinary dielectric-gated OFET, except for the difference with respect to the polarization characteristics of the gate insulator (a detailed description is given in Chapter 4). When a voltage is applied to the gate electrode of an electrolyte-gated OFET, electric double layers are formed along the two interfaces that are in contact with the electrolyte. These electric double layers are associated with a high capacitance per unit area, thus making low-voltage operation possible. One potential drawback with electrolyte-gated OFETs is that ions might penetrate into the organic semiconductor, resulting in electrochemical doping of the organic semiconductor bulk [25, 90]. In such case, the switching speed of the transistor is normally slow. Recently, *p*-channel OFETs gated via polyanion-based polyelectrolytes have been demonstrated [24, 26]. Electrochemical doping of the organic semiconductor in these transistors is prevented since the polyanions are immobile, meaning that they cannot penetrate into the semiconductor bulk. These transistors are operated at low voltages (< 1 V) with high output currents and exhibit fast turn-on and turn-off response (< 100 μ s) [91].

5.3. Supercapacitors

Electrical energy is commonly stored in batteries or conventional capacitors. Their energy storage and rate of charge delivery capability are specified in terms of the specific energy (energy per mass) and the specific power (power per mass) [92]. Batteries have typically much higher specific energy than conventional capacitors but on the other hand significantly lower specific power [93]. In other words, a battery can store much more energy in comparison to a capacitor but it cannot deliver it as fast. Supercapacitors (SCs), sometimes

also referred to as electrochemical capacitors or ultracapacitors, are promising energy storage devices that combine high power capability with high specific energy [94]. SCs are basically built up from two electrodes that are immersed in, or sandwiched around, an electrolyte. To avoid electrical shorting between the two electrodes an ion-permeable separator is sometimes incorporated between the electrodes. As for conventional capacitors, the energy (E) stored in a SC is given by Equation 5.15, where C is the capacitance and V is the voltage between the two electrodes.

$$E = \frac{CV^2}{2} \quad (5.15)$$

Clearly, both the capacitance, which describes the amount of charge stored by the electrodes per voltage unit; and, the applied voltage should be as high as possible in order to store as much energy as possible. The maximum operational voltage is limited by the electrochemical degradation of the electrolyte [95, 96]. This means that a larger stable potential window of the electrolyte will allow for a higher operational voltage of the SC. The maximum operational voltage of aqueous electrolytes is typically around 1 V, while it is considerably higher for non-aqueous electrolytes (~ 3 V) [93, 96, 97]. Thus, the specific energy of a SC can be increased almost by an order of magnitude, at a specific capacitance, by simply using a non-aqueous electrolyte instead of an aqueous electrolyte. However, most non-aqueous electrolytes have a much higher resistivity than aqueous electrolytes with the same ion concentration [98]. This leads to a significant increase of the equivalent series resistance (R_S) of the SC and a reduced maximum deliverable power (P_{Max}), given by Equation 5.16 [97].

$$P_{\text{Max}} = \frac{V^2}{4R_S} \quad (5.16)$$

Based on the mechanism of charge storage, SCs are commonly divided into two general classes; electric double layer capacitors and pseudo-capacitors [94, 99]. A third class, the hybrid capacitors, arises when the two former classes are combined [98]. The charge storage mechanism is described briefly for each of these three classes.

5.3.1. Electric double layer capacitors

Electric double layer capacitors are capacitors that store the charge in electric double layers. As described for electrolyte-based capacitors with planar metal electrodes in Chapter 4, the capacitance of an electric double layer is high (tens of $\mu\text{F}/\text{cm}^2$). This is a result of the very narrow charge separation between the ions and the charged electrode (a few Å). This narrow charge separation combined with (porous) electrodes having a high specific surface area (surface area per electrode mass) can result in “extremely” high values of the specific capacitance (capacitance per electrode mass; around 100 F/g [51, 96]) [100]. The most common choice of electrode material for this class of SCs is carbon in various forms; for instance activated carbons [101, 102] and carbon nanotubes (CNTs) [27, 103], as it combines a high specific surface area (up to $3000 \text{ m}^2/\text{g}$ [51]) with high electronic conductivity and also electrochemical stability. An illustration of an ideal porous electric double layer capacitor is given in Figure 5.6a. This SC consists of two porous networks of CNTs sandwiching an electrolyte. When a voltage is applied to the electrodes (Fig. 5.6b), ions migrate towards their oppositely charged electrode and form electric double layers at each of the two electrolyte-electrode interfaces.

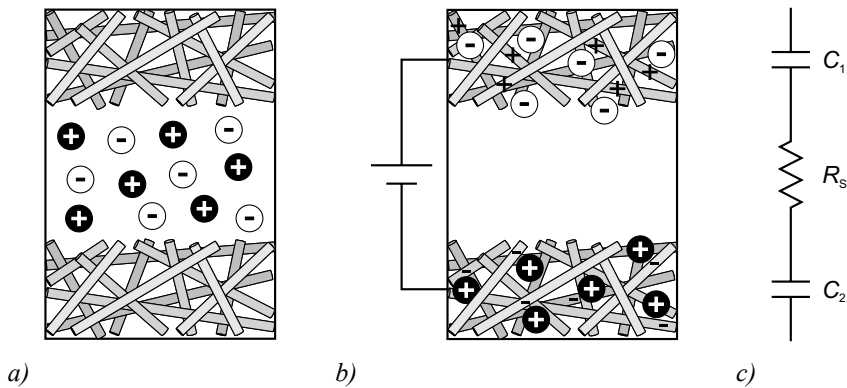


Figure 5.6. Idealized illustration of the charge storage mechanism in an electric double layer capacitor consisting of two high-surface area electrodes (two porous networks of CNTs) sandwiching an electrolyte. a) With no voltage applied, the ions in the electrolyte are randomly distributed. b) When a voltage is applied, ions migrate towards their oppositely charged CNT electrode and form electric double layers at the electrolyte-electrode interfaces. c) Electrical equivalent circuit of the supercapacitor.

In a simple electrical equivalent circuit of this SC, each of the two electrolyte-electrode interfaces is represented by a capacitor. These two capacitors are connected in series with the equivalent series resistance of the SC according to Figure 5.6c [92]. The total capacitance (C_{Tot}) of this equivalent circuit is obtained via Equation 5.17.

$$\frac{1}{C_{\text{Tot}}} = \frac{1}{C_1} + \frac{1}{C_2} \quad (5.17)$$

For a symmetric electric double layer capacitor, C_1 and C_2 are expected to be similar ($C_1 \approx C_2$) with $C_{\text{Tot}} \approx C_1/2$ [92]. Since two electrodes are needed for a capacitor, the total electrode mass is twice that of a single electrode. This means that the specific capacitance of a SC is one quarter of the specific capacitance of one of its electrodes [101]. Thus, it is important to indicate if the reported value of the specific capacitance corresponds to the value of the complete SC or to that of a single electrode. Note that if the capacitances of the two electrolyte-large-area electrode interfaces are not similar ($C_1 \neq C_2$), the total capacitance will be dominated by the interface associated with the lowest capacitance.

5.3.2. Pseudo-capacitors

In contrast to electric double layer capacitors, in which the charge storage mechanism is electrostatic, the charge storage mechanism in pseudo-capacitors involves electron transfer across the electrode-electrolyte interfaces [104]. This electron transfer results in a change of oxidation state in electrochemically active electrodes, and can give rise to a so-called pseudo-capacitance [97]. The pseudo-capacitance associated with a reduction-oxidation (redox) reaction is related to charge storage within the bulk of the redox active electrodes [105]. Two groups of materials have been investigated extensively as electrode material in pseudo-capacitors; metal oxides and conducting polymers (doped semiconducting polymers) [96].

Semiconducting polymers are electrochemically active materials into which electronic charge carriers, as mentioned in Chapter 2, can be introduced via electrochemical doping. A sandwich structure of a pseudo-capacitor that consists of two semiconducting polymer electrodes sandwiching an electrolyte is given in Figure 5.7a. There exist three different configurations of pseudo-capacitor devices with electrodes exclusively based on conducting polymers [15]. In the most attractive configuration, the same semiconducting neutral polymer

is used for both electrodes. This polymer can be *p*-doped (oxidized) and *n*-doped (reduced) within the stable potential window of the electrolyte.

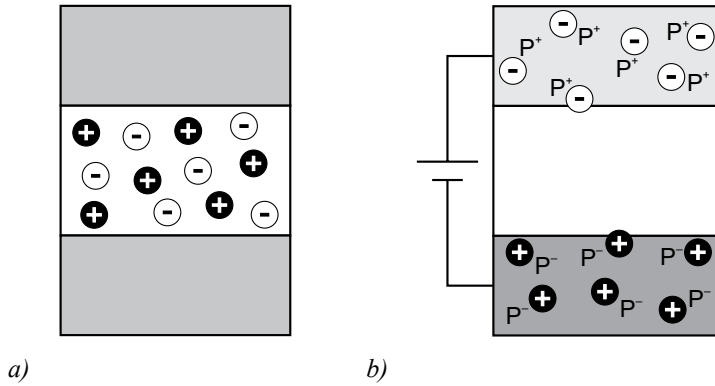
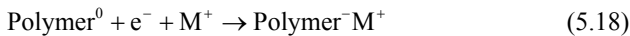


Figure 5.7. Idealized illustration of the charge storage mechanism in a pseudo-capacitor consisting of two semiconducting polymer electrodes sandwiching an electrolyte. This semiconducting polymer can be *p*-doped and *n*-doped. a) When no voltage is applied, the polymer electrodes are in their semiconducting neutral state and the ions are randomly distributed in the electrolyte. b) When a voltage is applied, the negatively biased polymer electrode becomes reduced (dark color) while the positively biased polymer electrode becomes oxidized (light color). Electroneutrality is maintained in both of the polymer electrodes by oppositely charged counter ions that migrate across the electrolyte-electrode interfaces to balance the polarons (P^+ and P^-) in the polymer electrodes.

When a voltage is applied to the SC (Fig. 5.7b), electrons are introduced into the π system of the negatively biased semiconducting polymer electrode. This polymer electrode becomes reduced (Eq. 5.18) and the negative polarons are balanced (to maintain electroneutrality) with positively charged counter ions (M^+) that migrate, from the electrolyte across the electrolyte-polymer electrode interface, into the polymer electrode [106].



Simultaneously; electrons are withdrawn from the π system of the positively biased semiconducting polymer electrode. This polymer electrode becomes oxidized (Eq. 5.19) and positive polarons are balanced by negatively charged counter ions (A^-).



Thus, with one polymer electrode in its *n*-doped (conducting) state and the other in its *p*-doped (conducting) state, ions are stored within the bulk of the polymer electrodes and this pseudo-capacitor configuration is in its charged state [107, 108]. When the SC is discharged, all the doping charge can be released and the two conducting polymer electrodes are oxidized and reduced, respectively, towards their fully discharged semiconducting state (reversed direction in Equations 5.18-5.19). However, difficulties related to the *n*-doping process, such as instability, need for negative potentials outside the stable potential window of the electrolyte and low specific capacitance; limit the actual performance of these pseudo-capacitors [105].

Since the total mass and volume of the polymer electrodes are involved in the pseudo-capacitor charge storage, higher values of the specific capacitance (~100-500 F/g) are commonly obtained for this SC class compared to electric double layer capacitors [105, 109]. However, the insertion and removal of counter ions into and out from the polymer electrodes during the doping processes degrades the polymer, which results in poor stability during cycling. Research related to conducting polymer-based SCs are currently directed towards hybrid capacitors.

5.3.3. Hybrid capacitors

Hybrid capacitors are SCs that combine the charge storage mechanisms of electric double layer capacitors and pseudo-capacitors. These SCs offers improved stability during cycling compared with pseudo-capacitors based on conducting polymers [110]. It has, for instance, been reported that in SCs with CNT-conducting polymer composite electrodes, the CNT network of each composite electrode serves as a conducting support that adapts to the mechanical stress associated with the doping processes of the polymer [109, 110]. In addition, as a result of the high surface area (provided by the CNT network) of the composite electrode, the specific capacitance of a SC with such composite electrodes can be even higher [111, 112].

In an asymmetric hybrid capacitor, one of the electrodes is an electric double layer capacitor electrode while the other is a pseudo-capacitor electrode. One successful way to overcome the problems related to the *n*-doped polymer electrode in the pseudo-capacitor configuration is to replace that electrode with a high-surface area carbon electrode [16, 113]. An asymmetric hybrid capacitor that consists of a semiconducting polymer electrode and an electrode of a

porous network of CNTs sandwiching an electrolyte is given in Figure 5.8a. With a positive voltage applied (Fig. 5.8b); an electric double layer is formed at the electrolyte-CNT electrode interface, while the polymer electrode becomes p -doped (Eq. 5.19). The positive polarons are balanced with negatively charged counter ions that migrate across the electrolyte-polymer interface into the polymer electrode to maintain electroneutrality. Thus, the electrostatic charge storage mechanism at the negatively biased CNT electrode-electrolyte interface is coupled to a pseudo-capacitive charge storage mechanism at the polymer electrode.

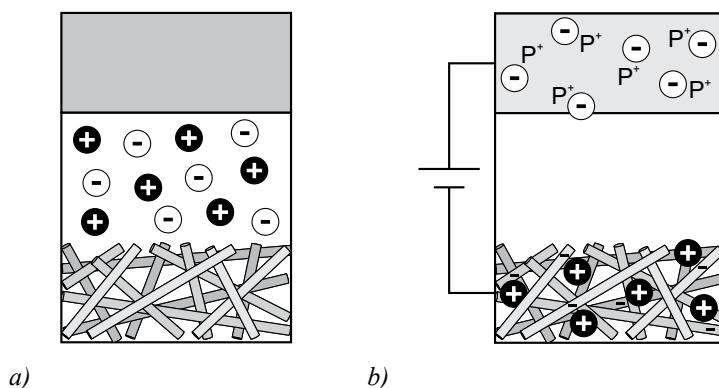


Figure 5.8. Idealized illustration of the charge storage mechanism in an asymmetric hybrid capacitor consisting of a semiconducting polymer electrode and a high-surface area electrode, here a porous network of CNTs, sandwiching an electrolyte. a) When no voltage is applied, the polymer electrode is in its semiconducting neutral state and the ions are randomly distributed in the electrolyte. b) When a positive voltage is applied, an electric double layer is formed at the CNT electrode while the polymer electrode becomes p -doped. Electroneutrality in the doped polymer electrode is maintained by negatively charged counter ions that migrate across the electrolyte-polymer interface to balance the polarons (P^+).

6. Conclusions and future outlook

The common point for the first four papers, despite the fact that one of them is related to sensors, two of them are related to transistors and one is related to supercapacitors, is that they are related to the polarization mechanisms of a polyelectrolyte in which the water content is varied. It was found that the polarization characteristics in a polyelectrolyte capacitor could be divided into three different frequency regions between 100 Hz and 1 MHz. At high frequencies a region attributed to dipolar relaxation in the polyelectrolyte, at intermediate frequencies a region attributed to ionic relaxation, and at low frequencies a region attributed to the formation of electric double layers at the polyelectrolyte-electrode interfaces. The transitions between regimes with different polarization mechanisms were shifted towards higher frequencies when the water content (proton conductivity) in the polyelectrolyte was increased.

The ionic relaxation in a polyelectrolyte was utilized as the sensing probe in a passively operated humidity sensor that was readout with a wireless technique. The production scheme of this sensor circuit is compatible with existing low-cost and high-volume manufacturing techniques, and can be integrated into a low-cost flexible electronic sensor label. This enables (humidity) sensing within new application areas that previously has been too expensive to monitor with existing sensor technologies. Such sensors can, for instance, be permanently mounted inside walls or beneath floors in houses and buildings for wireless monitoring of eventual leakage or moisture problems. Monitoring of the status of humidity-sensitive goods during transportation and storage, and drying processes inside materials are also possible applications. The polyelectrolyte used as the humidity-sensitive material in the presented sensors is soluble in water, which limits the humidity range for practical usage to lower humidity levels. However, this problem can be solved by different methods, for instance via copolymerization or cross-linking [114, 115]. On the other hand, a polyelectrolyte that becomes dissolved at high humidity levels gives the sensor a memory function that enables

the user to determine if the sensor has been exposed to a too high humidity level or not. Ongoing and future work relates to producing the complete sensor circuit entirely with low-cost manufacturing techniques on a single flexible substrate or label.

It was shown that the polarization of the polyelectrolyte limits the time response of polyelectrolyte-gated organic field-effect transistors with short channel lengths. The three different polarization mechanisms of the polyelectrolyte explained the evolution of the saturation current versus time for these transistors at low and moderate humidity levels. At high voltages, another phenomenon starts; the electrolysis of water. The impact of this electrochemical side reaction on the transistor characteristics has been investigated. It was shown that a large part of the leakage current originated from the electrolysis. Hence, this class of transistors should be operated in a dry environment or within the stable potential window of water. Surprisingly, even at low humidity levels, for which the ionic conductivity is significantly decreased, the transistors were able to respond quickly to the gate voltage. The transistors are expected to operate at even higher frequencies if the ionic mobility of the electrolyte is higher. This means that the ideal electrolyte for these transistors should be a solid electrolyte with high ionic mobility, even in dry environments. Recently, this class of transistors has been reported as promising candidates for low-voltage printed electronics applications [116].

A solid polyelectrolyte film was demonstrated as an effective ion-conducting medium for electric double layer supercapacitors. These supercapacitors were composed of two high-surface area electrodes of carbon nanotube (CNT) networks sandwiching the polyelectrolyte. It was found that the performance of the supercapacitors is limited by the ionic conductivity of the polyelectrolyte, rather than by the contact between the solid polyelectrolyte film and the CNT electrodes. High values of the specific capacitance (85 F/g at 80% relative humidity) were obtained as a result of the large effective electrode area of the CNT electrodes and the high ionic conductivity of the polyelectrolyte at high humidity levels. It has recently been demonstrated that CNT-based thin-film supercapacitors are very promising candidates as printed energy storage devices [27]. As solid polyelectrolytes combine the mechanical properties of polymers with the ionic conductivity of electrolytes, they are attractive for usage in such printed solid-state energy storage devices.

The fifth paper is related to the two previous papers concerning electrolyte-gated organic transistors. Two different types of transistors, both gated via an ordinary electrolyte and identical in terms of materials and structure except for their gate electrodes, were focused. It was demonstrated that the degree of advancement, or the extent, of an electrochemical reaction (oxidation) in the semiconducting polymer transistor channel is determined by the capacitance of the gate electrode. With a “low-capacitance” gate electrode, here a flat gold electrode, the extent of oxidation in the semiconductor was confined to the semiconducting polymer-electrolyte interface. This transistor operates in the “field-effect regime” with interfacial (two-dimensional) charge transport. This finding details the device mechanism of electrolyte-gated organic field-effect transistors. The other transistor type had a “high-capacitance” gate electrode; a high-surface area CNT network, thus connecting this paper with the work on supercapacitors as well. With the high-capacitance gate electrode, the oxidation of the polymer semiconductor was extended through the bulk; or in other words, the bulk of the semiconductor became electrochemically doped. As for polymer-based asymmetric hybrid supercapacitors, this electrochemical half-reaction was driven by the high electrostatic capacitance of the gate electrode. This transistor type operates in the “electrochemical regime” with bulk (three-dimensional) charge transport. Hence, it is crucial to take the nature of the charge transport into account when extracting the mobility. The methodology developed in this paper is expected to be useful for determining the device mechanism of electrolyte-gated organic transistors composed of other material combinations.

To conclude; the most important scientific insights of my research relate to the studies and characterization of the polarization characteristics in polyelectrolyte capacitors, and to the finding that the capacitance of the gate electrode determines the “regime” of transistor operation (field-effect or electrochemical) in electrolyte-gated organic transistors.

References

1. *The Nobel Prize*, <http://nobelprize.org>, accessed April 2011.
2. A. J. Heeger, *Journal of Physical Chemistry B* **2001**, *105*, 8475-8491.
3. J. H. Burroughes, D. D. C. Bradley, A. R. Brown, R. N. Marks, K. Mackay, R. H. Friend, P. L. Burns, A. B. Holmes, *Nature* **1990**, *347*, 539-541.
4. M. Berggren, O. Inganäs, G. Gustafsson, J. Rasmussen, M. R. Andersson, T. Hjertberg, O. Wennerström, *Nature* **1994**, *372*, 444-446.
5. A. Tsumura, H. Koezuka, T. Ando, *Applied Physics Letters* **1986**, *49*, 1210-1212.
6. G. Horowitz, *Advanced Materials* **1998**, *10*, 365-377.
7. H. Sirringhaus, *Advanced Materials* **2005**, *17*, 2411-2425.
8. C. J. Brabec, N. S. Sariciftci, J. C. Hummelen, *Advanced Functional Materials* **2001**, *11*, 15-26.
9. D. Nilsson, M. Chen, T. Kugler, T. Remonen, M. Armgarth, M. Berggren, *Advanced Materials* **2002**, *14*, 51-54.
10. D. Nilsson, N. Robinson, M. Berggren, R. Forchheimer, *Advanced Materials* **2005**, *17*, 353-358.
11. Q. Pei, G. Yu, C. Zhang, Y. Yang, A. J. Heeger, *Science* **1995**, *269*, 1086-1088.
12. J. H. Shin, N. D. Robinson, S. Xiao, L. Edman, *Advanced Functional Materials* **2007**, *17*, 1807-1813.
13. P. Andersson, D. Nilsson, P. O. Svensson, M. Chen, A. Malmström, T. Remonen, T. Kugler, M. Berggren, *Advanced Materials* **2002**, *14*, 1460-1464.

14. P. Tehrani, L. O. Hennerdal, A. L. Dyer, J. R. Reynolds, M. Berggren, *Journal of Materials Chemistry* **2009**, *19*, 1799-1802.
15. A. Rudge, J. Davey, I. Raistrick, S. Gottesfeld, J. P. Ferraris, *Journal of Power Sources* **1994**, *47*, 89-107.
16. A. Laforgue, P. Simon, J. F. Fauvarque, J. F. Sarrau, P. Lailier, *Journal of the Electrochemical Society* **2001**, *148*, A1130-A1134.
17. B. Adhikari, S. Majumdar, *Progress in Polymer Science* **2004**, *29*, 699-766.
18. Z. M. Rittersma, *Sensors and Actuators, A: Physical* **2002**, *96*, 196-210.
19. D. Nilsson, T. Kugler, P. O. Svensson, M. Berggren, *Sensors and Actuators, B: Chemical* **2002**, *86*, 193-197.
20. D. J. Macaya, M. Nikolou, S. Takamatsu, J. T. Mabeck, R. M. Owens, G. G. Malliaras, *Sensors and Actuators, B: Chemical* **2007**, *123*, 374-378.
21. T. Lindfors, A. Ivaska, *Analytica Chimica Acta* **2001**, *437*, 171-182.
22. J. Bobacka, A. Ivaska, A. Lewenstam, *Electroanalysis* **2003**, *15*, 366-374.
23. J. H. Cho, J. Lee, Y. Xia, B. Kim, Y. He, M. J. Renn, T. P. Lodge, C. D. Frisbie, *Nature Materials* **2008**, *7*, 900-906.
24. L. Herlogsson, X. Crispin, N. D. Robinson, M. Sandberg, O. J. Hagel, G. Gustafsson, M. Berggren, *Advanced Materials* **2007**, *19*, 97-101.
25. J. D. Yuen, A. S. Dhoot, E. B. Namdas, N. E. Coates, M. Heeney, I. McCulloch, D. Moses, A. J. Heeger, *Journal of the American Chemical Society* **2007**, *129*, 14367-14371.
26. E. Said, X. Crispin, L. Herlogsson, S. Elhag, N. D. Robinson, M. Berggren, *Applied Physics Letters* **2006**, *89*, 143507:1-3.
27. M. Kaempgen, C. K. Chan, J. Ma, Y. Cui, G. Grüner, *Nano Letters* **2009**, *9*, 1872-1876.
28. O. Larsson, *Polarization characteristics in polyelectrolyte thin film capacitors - Targeting field-effect transistors and sensors*, Licentiate thesis, Linköping University, **2009**.
29. M. Fahlman, W. R. Salaneck, *Surface Science* **2002**, *500*, 904-922.

30. A. K. Geim, K. S. Novoselov, *Nature Materials* **2007**, *6*, 183-191.
31. A. H. Castro Neto, F. Guinea, N. M. R. Peres, K. S. Novoselov, A. K. Geim, *Reviews of Modern Physics* **2009**, *81*, 109-162.
32. P. R. Wallace, *Physical Review* **1947**, *71*, 622-634.
33. P. Avouris, Z. Chen, V. Perebeinos, *Nature Nanotechnology* **2007**, *2*, 605-615.
34. H.-S. Philip Wong, D. Akinwande, *Carbon Nanotube and Graphene Device Physics*, Cambridge University Press, Cambridge, **2011**.
35. S. Iijima, T. Ichihashi, *Nature* **1993**, *363*, 603-605.
36. D. S. Bethune, C. H. Kiang, M. S. de Vries, G. Gorman, R. Savoy, J. Vazquez, R. Beyers, *Nature* **1993**, *363*, 605-607.
37. S. Iijima, *Nature* **1991**, *354*, 56-58.
38. R. Waser, *Nanoelectronics and Information Technology - Advanced Electronic Materials and Novel Devices*, Wiley, Weinheim, **2003**.
39. R. L. McCreery, *Chemical Reviews* **2008**, *108*, 2646-2687.
40. W. Zhou, X. Bai, E. Wang, S. Xie, *Advanced Materials* **2009**, *21*, 4565-4583.
41. L. X. Zheng, M. J. O'Connell, S. K. Doorn, X. Z. Liao, Y. H. Zhao, E. A. Akhadov, M. A. Hoffbauer, B. J. Roop, Q. X. Jia, R. C. Dye, D. E. Peterson, S. M. Huang, J. Liu, Y. T. Zhu, *Nature Materials* **2004**, *3*, 673-676.
42. R. Saito, M. Fujita, G. Dresselhaus, M. S. Dresselhaus, *Applied Physics Letters* **1992**, *60*, 2204-2206.
43. J. W. G. Wildöer, L. C. Venema, A. G. Rinzler, R. E. Smalley, C. Dekker, *Nature* **1998**, *391*, 59-62.
44. T. W. Odom, J. L. Huang, P. Kim, C. M. Lieber, *Nature* **1998**, *391*, 62-64.
45. Q. Cao, J. A. Rogers, *Advanced Materials* **2009**, *21*, 29-53.
46. S. Roth, H. J. Park, *Chemical Society Reviews* **2010**, *39*, 2477-2483.
47. N. Saran, K. Parikh, D. S. Suh, E. Muñoz, H. Kolla, S. K. Manohar, *Journal of the American Chemical Society* **2004**, *126*, 4462-4463.

48. J. Li, L. Hu, L. Wang, Y. Zhou, G. Grüner, T. J. Marks, *Nano Letters* **2006**, *6*, 2472-2477.
49. E. S. Snow, J. P. Novak, P. M. Campbell, D. Park, *Applied Physics Letters* **2003**, *82*, 2145-2147.
50. L. Hu, D. S. Hecht, G. Grüner, *Chemical Reviews* **2010**, *110*, 5790-5844.
51. L. L. Zhang, X. S. Zhao, *Chemical Society Reviews* **2009**, *38*, 2520-2531.
52. C. H. Hamann, A. Hamnett, W. Vielstich, *Electrochemistry*, Wiley, Weinheim, **1998**.
53. F. M. Gray, *Polymer Electrolytes*, The Royal Society of Chemistry, Cambridge, **1997**.
54. J. R. Macdonald, *Impedance Spectroscopy: Emphasizing Solid Materials and Systems*, Wiley, New York, **1987**.
55. S. M. Park, J. S. Yoo, *Analytical Chemistry* **2003**, *75*, 455-461.
56. A. J. Bard, L. R. Faulkner, *Electrochemical Methods: Fundamentals and Applications*, Wiley, New York, **2001**.
57. J. Bisquert, *Electrochimica Acta* **2002**, *47*, 2435-2449.
58. P. Colomban, *Proton Conductors*, Cambridge University Press, Cambridge, **1992**.
59. K. S. Cole, R. H. Cole, *Journal of Chemical Physics* **1941**, *9*, 341-351.
60. P. Lorrain, D. R. Corson, *Electromagnetism: Principles and Applications*, Freeman, New York, **1997**.
61. P. Atkins, J. d. Paula, *Atkin's Physical Chemistry*, Oxford University Press, Oxford, **2006**.
62. F. Bordi, C. Cametti, R. H. Colby, *Journal of Physics Condensed Matter* **2004**, *16*, 1423-1463.
63. Y. Sakai, Y. Sadaoka, M. Matsuguchi, *Sensors and Actuators, B: Chemical* **1996**, *35-36*, 85-90.
64. Z. Chen, C. Lu, *Sensor Letters* **2005**, *3*, 274-295.
65. Y. Li, M. J. Yang, Y. She, *Sensors and Actuators, B: Chemical* **2005**, *107*, 252-257.

66. G. Casalbore-Miceli, A. Zanelli, A. W. Rinaldi, E. M. Girotto, M. J. Yang, Y. S. Chen, Y. Li, *Langmuir* **2005**, *21*, 9704-9708.
67. G. Casalbore-Miceli, M. J. Yang, N. Camaioni, C. M. Mari, Y. Li, H. Sun, M. Ling, *Solid State Ionics* **2000**, *131*, 311-321.
68. P. M. Harrey, B. J. Ramsey, P. S. A. Evans, D. J. Harrison, *Sensors and Actuators, B: Chemical* **2002**, *87*, 226-232.
69. Y. Li, M. J. Yang, N. Camaioni, G. Casalbore-Miceli, *Sensors and Actuators, B: Chemical* **2001**, *77*, 625-631.
70. K. G. Ong, C. A. Grimes, *Smart Materials and Structures* **2000**, *9*, 421-428.
71. T. J. Harpster, B. Stark, K. Najafi, *Sensors and Actuators, A: Physical* **2002**, *95*, 100-107.
72. J. B. Ong, Z. You, J. Mills-Beale, E. L. Tan, B. D. Pereles, K. G. Ong, *IEEE Sensors Journal* **2008**, *8*, 2053-2058.
73. A. Facchetti, M. H. Yoon, T. J. Marks, *Advanced Materials* **2005**, *17*, 1705-1725.
74. J. Zaumseil, H. Sirringhaus, *Chemical Reviews* **2007**, *107*, 1296-1323.
75. S. M. Sze, *Physics of Semiconductor Devices*, Wiley, New York, **1981**.
76. H. Sirringhaus, P. J. Brown, R. H. Friend, M. M. Nielsen, K. Bechgaard, B. M. W. Langeveld-Voss, A. J. H. Spiering, R. A. J. Janssen, E. W. Meijer, P. Herwig, D. M. De Leeuw, *Nature* **1999**, *401*, 685-688.
77. R. J. Kline, M. D. McGehee, E. N. Kadnikova, J. Liu, J. M. J. Fréchet, *Advanced Materials* **2003**, *15*, 1519-1522.
78. J. F. Chang, B. Sun, D. W. Breiby, M. M. Nielsen, T. I. Sölling, M. Giles, I. McCulloch, H. Sirringhaus, *Chemistry of Materials* **2004**, *16*, 4772-4776.
79. L. A. Majewski, R. Schroeder, M. Grell, *Advanced Materials* **2005**, *17*, 192-196.
80. C. D. Dimitrakopoulos, S. Purushothaman, J. Kymissis, A. Callegari, J. M. Shaw, *Science* **1999**, *283*, 822-824.
81. M. Halik, H. Klauk, U. Zschieschang, G. Schmid, C. Dehm, M. Schütz, S. Malsch, F. Effenberger, M. Brunnbauer, F. Stellacci, *Nature* **2004**, *431*, 963-966.

82. L. A. Majewski, R. Schroeder, M. Grell, *Advanced Functional Materials* **2005**, *15*, 1017-1022.
83. H. G. O. Sandberg, T. G. Bäcklund, R. Österbacka, H. Stubb, *Advanced Materials* **2004**, *16*, 1112-1115.
84. T. G. Bäcklund, H. G. O. Sandberg, R. Österbacka, H. Stubb, *Applied Physics Letters* **2004**, *85*, 3887-3889.
85. A. S. Dhoot, J. D. Yuen, M. Heeney, I. McCulloch, D. Moses, A. J. Heeger, *Proceedings of the National Academy of Sciences of the United States of America* **2006**, *103*, 11834-11837.
86. M. J. Panzer, C. R. Newman, C. D. Frisbie, *Applied Physics Letters* **2005**, *86*, 103503: 1-3.
87. M. J. Panzer, C. D. Frisbie, *Journal of the American Chemical Society* **2005**, *127*, 6960-6961.
88. M. J. Panzer, C. D. Frisbie, *Journal of the American Chemical Society* **2007**, *129*, 6599-6607.
89. M. J. Panzer, C. D. Frisbie, *Advanced Materials* **2008**, *20*, 3176-3180.
90. L. G. Kaake, Y. Zou, M. J. Panzer, C. D. Frisbie, X. Y. Zhu, *Journal of the American Chemical Society* **2007**, *129*, 7824-7830.
91. L. Herlogsson, Y. Y. Noh, N. Zhao, X. Crispin, H. Sirringhaus, M. Berggren, *Advanced Materials* **2008**, *20*, 4708-4713.
92. M. Winter, R. J. Brodd, *Chemical Reviews* **2004**, *104*, 4245-4269.
93. R. Kötz, M. Carlen, *Electrochimica Acta* **2000**, *45*, 2483-2498.
94. A. G. Pandolfo, A. F. Hollenkamp, *Journal of Power Sources* **2006**, *157*, 11-27.
95. M. Ue, K. Ida, S. Mori, *Journal of the Electrochemical Society* **1994**, *141*, 2989-2996.
96. P. Simon, Y. Gogotsi, *Nature Materials* **2008**, *7*, 845-854.
97. B. E. Conway, *Electrochemical Supercapacitors - Scientific Fundamentals and Technological Applications*, Kluwer Academic/Plenum Publishers, New York, **1999**.
98. A. Burke, *Journal of Power Sources* **2000**, *91*, 37-50.

99. A. S. Aricò, P. Bruce, B. Scrosati, J. M. Tarascon, W. van Schalkwijk, *Nature Materials* **2005**, *4*, 366-377.
100. A. K. Shukla, S. Sampath, K. Vijayamohanan, *Current Science* **2000**, *79*, 1656-1661.
101. D. Qu, H. Shi, *Journal of Power Sources* **1998**, *74*, 99-107.
102. E. Frackowiak, F. Béguin, *Carbon* **2001**, *39*, 937-950.
103. C. Niu, E. K. Sichel, R. Hoch, D. Moy, H. Tennent, *Applied Physics Letters* **1997**, *70*, 1480-1482.
104. B. E. Conway, V. Birss, J. Wojtowicz, *Journal of Power Sources* **1997**, *66*, 1-14.
105. G. A. Snook, P. Kao, A. S. Best, *Journal of Power Sources* **2011**, *196*, 1-12.
106. A. Laforgue, P. Simon, C. Sarrazin, J. F. Fauvarque, *Journal of Power Sources* **1999**, *80*, 142-148.
107. C. Arbizzani, M. Mastragostino, L. Meneghello, *Electrochimica Acta* **1996**, *41*, 21-26.
108. M. Hughes, G. Z. Chen, M. S. P. Shaffer, D. J. Fray, A. H. Windle, *Chemistry of Materials* **2002**, *14*, 1610-1613.
109. E. Frackowiak, V. Khomenko, K. Jurewicz, K. Lota, F. Béguin, *Journal of Power Sources* **2006**, *153*, 413-418.
110. K. Lota, V. Khomenko, E. Frackowiak, *Journal of Physics and Chemistry of Solids* **2004**, *65*, 295-301.
111. K. Jurewicz, S. Delpeux, V. Bertagna, F. Béguin, E. Frackowiak, *Chemical Physics Letters* **2001**, *347*, 36-40.
112. K. H. An, K. K. Jeon, J. K. Heo, S. C. Lim, D. J. Bae, Y. H. Lee, *Journal of the Electrochemical Society* **2002**, *149*, A1058-A1068.
113. J. H. Park, O. O. Park, *Journal of Power Sources* **2002**, *111*, 185-190.
114. M. S. Gong, J. S. Park, M. H. Lee, H. W. Rhee, *Sensors and Actuators, B: Chemical* **2002**, *86*, 160-167.
115. X. Lv, Y. Li, P. Li, M. Yang, *Sensors and Actuators, B: Chemical* **2009**, *135*, 581-586.

116. L. Herlogsson, M. Cölle, S. Tierney, X. Crispin, M. Berggren, *Advanced Materials* **2010**, *22*, 72-76.